Cell Host & Microbe

Innovative anti-cytolytic screen identifies potent inhibitors of mycobacterial virulence protein secretion

--Manuscript Draft--

Manuscript Number:	CELL-HOST-MICROBE-D-14-00341R1
Full Title:	Innovative anti-cytolytic screen identifies potent inhibitors of mycobacterial virulence protein secretion
Article Type:	Resource Article
Keywords:	Tuberculosis, protein secretion, ESX-1 system
Corresponding Author:	Stewart Cole, Ph.D. Lausanne, FRANCE
First Author:	Jan Rybniker
Order of Authors:	Jan Rybniker
	Jeffrey Chen
	Claudia Sala
	Ruben Hartkoorn
	Anthony Vocat
	Andrej Benjak
	Stefanie Boy-Röttger
	Ming Zhang
	Rita Szekely
	Zoltán Greff
	László Örfi
	István Szabadkai
	János Pató
	György Kéri
	Stewart Cole, Ph.D.
Abstract:	Mycobacterium tuberculosis (Mtb) depends on protein secretion systems like ESX-1 for intracellular survival and virulence. The major virulence determinant and ESX-1-substrate, EsxA, causes tissue damage and necrosis, thereby promoting pathogen spread and dissemination. We developed a fibroblast survival assay (FSA) that exploits this phenotype by selecting for molecules that protect host cells from Mtb-induced lysis without being bactericidal in vitro. Hit compounds identified in this high-throughput screen blocked secretion of EsxA thus promoting phagosome maturation and substantially reducing bacterial burden in activated macrophages. Target identification studies led to the discovery of BTP15, a benzothiophene inhibitor of the histidine kinase MprB that indirectly regulates ESX-1, and BBH7, a benzyloxybenzylidine hydrazine compound. BBH7 affects metal ion homeostasis in Mtb and revealed zinc stress as a signal for EsxA secretion. This novel screening approach extends the target spectrum of small molecule libraries and will help to tackle the mounting problem of antibiotic-resistant mycobacteria.
Suggested Reviewers:	Olivier Neyrolles olivier.neyrolles@ipbs.fr Expert in intracellular pathogenesis of TB and heavy metal toxicity
	Charles Thompson

	Expert in drug discovery and natural products with deep knowledge of actinobacteria
	Wilbert Bitter w.bitter@vumc.nl Expert in type 7 secretion systems and mycobacteriology
	Vojo Deretic vderetic@salud.unm.edu Expert in intracellular pathogenesis, autophagy and two component systems, particularly MprAB.
	Patricia Champion champion.7@nd.edu Expert in type 7 secretion systems and mycobacteria
	Miriam Braunstein braunste@med.unc.edu Expert in protein secretion
	Sophie Lagrange Sophie.Lagrange@sanofi.com Expert in screening, drug discovery and drug development
Opposed Reviewers:	Jeffery Cox Jeffery.Cox@ucsf.edu Potential conflict of interest

FACULTE DES SCIENCES DE LA VIE
GLOBAL HEALTH INSTITUTE
UNITE DU PROFESSEUR COLE

EPFL SV / GHI / UPCOL
SV 3531
Station n°19
CH-1015 Lausanne

Téléphone : +4121 693 1851
Fax : +4121 693 1790
E-mail : stewart.cole@epfl.ch
Site web : http://ghi.epfl.ch

ÉCOLE POLYTECHNIQUE
FÉDÉRALE DE LAUSANNE

Lausanne, 19 August 2014

Ella Hinson, Ph.D.
Scientific Editor
Cell Host & Microbe

Re. CELL-HOST-MICROBE-D-14-00341

Dear Dr. Hinson,

Thank you very much for sending the very positive reviews of our "Resource" paper that we have revised along the lines suggested by the reviewers.

Major changes to the manuscript are highlighted in the text whereas minor edits and shortening of the text are not. The manuscript currently contains 54,226 characters including spaces.

Detailed responses to the reviewers' queries may be found in the accompanying rebuttal and we are confident that their comments have been more than adequately addressed by additional experimentation and careful editing of the text.

We would like to thank the reviewers for their helpful comments and constructive criticism, and you for handling the manuscript, which we trust will now be found acceptable for publication.

Since it was first submitted the authors have decided to file a patent to protect some of the compounds discussed in the paper. The filing has not yet been completed so I would like to request that the paper not be published online following acceptance if this is your policy. Thank you for considering this request and for providing a "conflict of interest form" for us to sign.

Sincerely yours,

Professor Stewart Cole FRS
Director of the Global Health Institute

Rebuttal CELL-HOST-MICROBE-D-14-00341

Reviewers' Comments:

Reviewer #1: The manuscript of Rybniker et al describes an elegant and interesting study for new compounds blocking M. tuberculosis virulence. They have developed and used a novel assay for this, by blocking the virulence mechanism of the crucial ESX-1 system. Using this system the authors have identified two new classes of compounds with interesting activities. Overall, the manuscript is interesting, novel and well written and as such important for the field and for a wider audience. Suggestions for improvement:

The authors indicate that BTP15 could function as a kinase inhibitor through inhibition of the autophosphorylation of MprB, resulting in altered expression of espA. However, the difference in expression of espA is rather mild (factor 2) and also an espA mutant (fig. 1B) seems to have a more mild effect than compound BTP15. The authors should discuss these observations, which probably mean that the regulon of MprB could potentially contain more genes that have an influence on ESX-1 functioning.

*We agree with reviewer 1 that dysregulation of the espACD operon alone would not fully explain the strong attenuation of BTP15-treated bacteria since the ΔespA strain is only moderately attenuated in the FSA. We have recently shown that stronger (BTP15-like) attenuation requires both dysregulation of the espACD regulon AND the ESX-1 core region (Chen et al., Mol. Micro. 2013). A typical sign for dysregulation of the ESX-1 core region is inhibition of EspB secretion, a core protein that is still secreted in the espACD mutant (Chen et al., Mol. Micro. 2013). Interestingly, the ΔmprAB mutant is also defective in EspB secretion (Pang et al. JB, 195, 66-75, 2013). Furthermore, putative MprA binding sites have been identified in the esxA promoter (RD1 region). The whiB6 gene, which is involved in RD1 gene regulation, is also under control of MprA (Pang et al. JB, 195, 66-75, 2013, Pang et al. Microbiology 153, 3007). This indicates that MprAB not only regulates the espACD operon but also the ESX-1 core region. In the revised manuscript we included an anti-EspB Western blot of BTP1-treated samples showing that EspB-secretion is also affected by this compound (new Figure S3B), which explains the strong attenuation of BTP15-treated bacteria. This is discussed in the revised manuscript lines 328 – 332: "*MprAB also seems to regulate the ESX-1 region itself since the *mprAB* mutant fails to secrete EspB, a protein that is not influenced by the *espACD* operon (Chen et al., 2013; Pang et al., 2013). We also found inhibition of EspB secretion upon BTP15 treatment (Figure S3B), accompanied by greater attenuation than seen with a Δ*espA* mutant in the FSA."

The authors convincingly show that compound BBH7 affects cell wall permeability using the EtBr assay. However, it would be interesting to determine whether also sensitivity to other antibiotics is altered due to this permeability defect.

*In the revised version of the manuscript we present the results of testing a panel of antimycobacterial drugs in the presence of 0, 10 and 25 µM of BBH7. Interestingly, the MIC of these compounds was not altered in the presence of these rather high concentrations of BBH7 in contrast to treatment of Mtb with broadly acting efflux pump inhibitors or protonophores such as CCCP, which have a major impact on MICs of anti-TB drugs (Rodrigues et al., BMC Microbiology 11:35, 2011; Gupta et al. Microbial Drug Resistance, Vol 16, 1, 2010). This indicates that BBH7-induced cell wall alterations are subtle leading to accumulation of selected molecules such as the cationic dye EtBr and well-defined alterations of the mycobacterial transcriptome (metal ion stress). However, this subtle alteration has a major impact on the intracellular survival of Mtb probably due to the effect on virulence protein secretion. The new data were added to the supplementary information (Figure S5) and to the main text, lines 246 – 247: "*Interestingly, BBH7 concentrations as high as 25 µM had no impact on the activity of first- and second-line TB drugs (Figure S5).*"*

Furthermore, and perhaps more importantly, the authors mention that the alteration in cell wall permeability are leading to signs or zinc and copper stress (line 261). However, in my opinion the authors should be careful to what is the cause and the consequence of cell wall permeability, gene induction and zinc/copper stress. Zinc stress could also be achived for instance by blocking the ESX-3 secretion system (which should be mentioned).

*Several publications link the essential ESX-3 system with iron and zinc stress and we agree with reviewer 1 that alterations of ESX-3 secretion through BBH7 may lead to transcriptional signs of zinc stress. Although we were unable to identify differential secretion of the ESX-3 substrates EsxG/H (which carry a zinc binding site) in the mycobacterial secretome (see comment below), we did see down-regulation of the respective genes upon treatment (Figure 5, Table S3). This correlates well with published data showing that ESX-3 depletion leads to up-regulation of genes associated with zinc starvation (Serafini et al, PLOSone Vol8/10, 2013). Thus, the ESX-3 system responds to BBH7 treatment, but it is not known whether this happens in response to increased zinc levels in the mycobacterial cytosol or to direct alterations of ESX-3 through BBH7. Since ESX-3 seems to be involved in zinc uptake (depletion of ESX-3 leads to low intracellular zinc concentrations), blockage of ESX-3 by a small molecule will probably not lead to zinc accumulation as suggested by our RNA-seq data. Thus, it will rather be an increase of EsxG/H secretion that would cause the effects we saw for BBH7. We now discuss a possible role of ESX-3 and BBH7 function in lines 402 – 405: "*Of note, there is evidence that the ESX-3 secretion system is involved in zinc homeostasis of *Mtb* (Serafini et al., 2013). Thus, interference with ESX-3 activity by BBH7 may cause for the zinc stress observed.*"*

*- and have modified the sentence in lines 249 - 251 (previously 261) - this now reads: "*Having established that BBH7 treatment leads to transcriptional signs of zinc and copper stress, we surmised that intracellular metal-ion stress might be the link to inhibition of mycobacterial protein secretion.*"*

In Table S2 a number of proteins are listed that show reduced secretion upon addition of BBH7. However, the fold reduction is not shown and also a list of proteins that are not affected by the compound would be helpful to understand the mechanism of action, i.e. are all ESX-1 and ESX-5

substrates blocked? Is also the secretion of all extracellular proteins with a signal sequence blocked? Please also note that cut 3 has been suggested previously as a putative ESX-5 substrate (Abdallah et al., 2009).

In the revised version of Table S2 we now display the ratios of treated and untreated samples. For all of the chosen proteins, the amount of protein in the treated sample is heavily reduced.

In our MS experiments, we were able to identify 1140 proteins in the culture filtrate of Mtb. Approximately 5% of these were quantified with lower amounts in the BBH7-treated samples. We were unable to show reduced secretion of all ESX-1 substrates. EspA and EspC for example were not significantly reduced upon treatment. However, due to strong reduction of overall protein content in BBH7-treated culture filtrate (approx. 50% less total protein) it was difficult to normalize the MS data against the background. This led to a relatively stringent statistical data evaluation with better identification of differential secretion of the most abundant proteins. EspA and EspC are not very abundant and though there was a clear trend towards reduction of these proteins in the treated samples, the p-value was not below the threshold of 0.05. This also applies to Tat secreted proteins.Ag85C carries a signal sequence for Tat secretion – this protein was clearly reduced in the treated samples. However, Ag85A, another Tat substrate, was significantly reduced in the forward experiment (p-value <0.05) but not in the reverse experiment (p-value = 0.06).

We performed the MS experiments primarily to confirm Western blot data, which indicated that the secretion of non-ESX-1 substrates is also affected by BBH7. We were able to identify at least 3 secretion systems that were significantly affected: ESX-1, ESX-5 and Tat. However, the strong effect of BBH7 on protein secretion heavily impairs the protein ratio density and thereby reduces the efficiency of statistical tools in detecting changes to all proteins.

The reference to cut3 has now been changed to ESX-5.

Please check the use of that/which.

This has been checked and some changes made.

Reviewer #2: This paper describes an anti-cytolytic screen conducted in MRC-5 lung fibroblasts infected with high doses of Mycobacterium tuberculosis (M.tb). The innovative aspect of this study is the identification of M.tb secreted proteins by screening for compounds that inhibit M.tb cytotoxicity in fibroblasts but are not bactericidal in vitro. The authors focus on inhibition of Esx-1 (ESAT-6), a secreted mycobacterial protein involved in membrane binding and host cell lysis. An input library of over 10,000 compounds yielded benzothiophene inhibitors and benzyloxybenzylidine hydrazine as two major classes of compounds that met hit criteria. The authors subsequently investigated the possible mechanism of action for two compounds with M.tb specific activity: BTP15 and BBH7. While they do not find a specific mode of action for BBH7, they do uncover a potential role for zinc as a signal for Esx1 secretion.

In general, the work is well done and the results are interesting. There is an unusual mix here - although labeled as a "resource" paper, much of the work involves investigating the mechanism of action of the compounds that they found in their screen, less of a resource and more of a science paper. However, whatever the designation, the results are interesting and publishable.

A couple of major items might make the work a bit more readable:

- The fibroblast assay will seem quite peculiar to those in the field and immediately raise red flags as there is little evidence that these are actually infected in vivo (and the MOI is certainly likely to be non physiologic). It would probably be worth framing the discussion around using these as a bioassay for ESX-1 function rather than infection. This seemed to be the intention and the fibroblasts probably offer advantages over screening in macrophages (although, what those are should be enumerated).

*We agree with reviewer 3 that the in vivo role of lung fibroblasts in mycobacterial pathogenesis is unknown although these cells are part of the Mtb-granuloma. In fact, in our screening assay the only purpose of these cells is quantification of Mtb induced cell-death. Though this works equally well with macrophages, one advantage of fibroblasts over these professional phagocytes is the failure to detect effects of host-modifying drugs like imatinib when using fibroblasts (see also comment 2 of the minor points). We tried to set up the assay in a sufficiently broad manner to target virtually all structural and regulatory ESX-1-components yet to be specific enough to exclude compounds with no or minor effects on this system (such as kinase inhibitors acting on the host), which makes target identification easier. This is now discussed in lines 310 – 314: "*Another key factor for selectivity of the bioassay is our choice of lung fibroblasts for the quantification of *Mtb*-induced cell death. These non-professional phagocytes fail to detect host modifying agents that reduce the intracellular burden of *Mtb* in macrophages (Lechartier et al., 2014). This feature may be beneficial for target identification of these anti-virulence drugs.*"*

- The confirmatory macrophage assays represent something a bit more like a real infection. These should be featured more prominently in both the results and discussion.

This wise suggestion has been followed. We have modified the results section of the macrophage experiments by linking it to the intracellular Mtb-quantification data generated in fibroblasts (Figure 2D) and changed the presentation of Figure 6 to make it more readable. Highlighting the difference in intracellular survival of BTP15-treated bacteria in fibroblasts vs. macrophages puts more emphasis on the importance of data generated in the activated THP-1 cells. All macrophage data are now presented in the main manuscript in lines 277 – 294 and not in the supplementary data section thereby ensuring greater prominence. Furthermore, the data are now referred to in the discussion lines 322 - 340.

- This might be a semantic point but I found it quite distracting. The compounds the authors describe are not clearly direct inhibitors of protein secretion. To the extent that their mechanism is clear, they produce broad transcriptional changes altering the production of some secreted proteins and of other proteins required for secretion. I find the title to be misleading.

We respectfully disagree with the reviewer and have retained the original title. At no point, do we state that the inhibitors directly target the protein secretion systems and on several occasions we indicate that BTP15 acts on an upstream kinase, MprB. Since we are not misleading the reader and the other reviewers had no objection to the wording of the title we feel that our choice is justified.

Minor points:

1. The authors do an excellent job of describing the screen that pairs the fibroblast survival assay (FSA) with the resazurin reduction microtiter assay (M.tb REMA). They are missing a citation for the original fibroblast assay describing correlation between MOI and cytotoxicity by Takii et. al (AAC, 2002).

We have included this citation in line 104 of the revised version of the manuscript as well as the Hsu et al. 2003 citation as requested by reviewer 3.

2. The authors highlight one limitation of the FSA when they show that compounds blocking host components of programmed cell death fail to protect M.tb infected fibroblasts from lysis, even though they have been shown to do this in infected macrophages. While this is designed to be a rapid screen, with only 3 days incubation with infected fibroblasts, it would be useful to see a longer time course and potential interactions between host-modifying compounds and infected fibroblasts.

As suggested by the reviewer we repeated the FSA using lower MOIs (5 and 2 instead of 10) and a longer incubation time of 5 days instead of 3 days. At an MOI of 5, the panel of host modifying agents had no effect on fibroblast survival (not shown). At an MOI of 2 there was only a slight protective effect of imatinib, the Akt inhibitor H-89 and AX20017 (but not of nilotinib – another BCR-Abl inhibitor). This stands in contrast to macrophage data where similar compounds had potent impact on intracellular Mtb burden (between 0.5 and 1 log reduction for imatinib), which most likely correlates with good survival of infected macrophages. Thus we assume that the inactivity of these compounds in the FSA is primarily due to the choice of fibroblasts, which are not professional phagocytes, and to differences in cell differentiation between the respective cell lines. This is discussed in lines 123 - 126 of the revised version: "Reducing the MOI led to a minor protective effect of some kinase inhibitors (Figure S1A) indicating that their inactivity in the FSA is primarily due to the choice of cell: fibroblasts versus macrophages."

and the new data may be found in Figure S1A.

3. Figure 2D shows that BTP15 is not toxic to GFP-M.tb in lung fibroblasts while BBH7 is. While this begins to show the different mechanisms of action of each drug, this experiment should be linked in the text to the comparable experiment done in macrophages in Figure 6C.

In the revised version of the manuscript we linked the experiment presented in Figure 2D with the section on macrophage experiments by recalling the fibroblast work at the beginning of the section presenting the macrophage results - lines 279 – 280: "Using GFP-expressing *Mtb* we had shown that BBH7 strongly affects viability of intracellular bacteria in MRC-5 fibroblasts whereas BTP15 does not (Figure 2D). "

4. The authors show clearly that treatment with BBH7 results in a dose-dependent inhibition of EsxA and Ag85 secretion, while BTP15 shows inhibition of EsxA and Ag85, but with a different pattern. Bacteria were grown in Sauton's medium for preparation of protein lists for the immunoblots, which nicely shows the efficacy of the compounds in different media.

We thank the reviewer for appreciating this point.

5. The authors show that mprA mRNA levels are downregulated with BTP15 treatment at late timepoints, and then further pursue an argument for deregulation of the mprAB locus leading to reduced EsxA secretion. Were mRNA levels of mprB also downregulated?

*Yes, this was the case. We found a 3-fold reduction in abundance of the mprB transcript after 48 hours of treatment with 10 µM of BTP15. This new set of data may be found in Figure S3A and lines 186 -187 of the main text: "*BTP15 (10 µM) also decreased *mprB* transcript levels 3-fold after 48 h exposure (Figure S3A)."

6. EtBr assays are used to study membrane permeability as well as efflux. The authors conclude that the increased fluorescence curve acquired with BBH7 treatment is suggestive of a change in membrane permeability. If the authors add an efflux pump inhibitor to the system, does the fluorescence shift?

The EtBr assay we describe has been extensively used by several groups to determine efflux and altered cell wall permeability in mycobacteria (Rodrigues et al. AAC, vol 57/2, 2013; Rodrigues et al., BMC microbiology 11:35, 2011, Machado et al. PLOSone, vol 7/4, 2012). It was shown that efflux pump inhibitors as well as ionophores that alter cell wall permeability lead to EtBr accumulation. Since this has been extensively documented already we decided not to repeat the experiment using pump inhibitors such as verapamil. Furthermore, the EtBr assay cannot differentiate between altered influx or efflux across the mycobacterial cell wall. In the case of BBH7, the transcriptomic signature shows signs of metal ion accumulation and this could also be due to reduced efflux of these ions. Thus, in our manuscript, we use the expression "altered cell wall permeability" and prefer not to use the terms "efflux" or "influx". Of note, when we screened a panel of FDA-approved drugs such as verapamil in the FSA, there was no protective effect on fibroblast survival. In addition, BBH7 had no impact on the MIC of a panel of antimycobacterial drugs, which stands in contrast to treatment with efflux pump inhibitors (new Figure S5 in the revised manuscript).

7. The authors use microscopy to show that there is a reduced bacterial load in the macrophage upon treatment with BBH7 and BTP15. However, since this paper has focused on the Esx1 secretion system, it would be nice to se a comparison experiment with a GFP-labeled ESX1 knockout strain.

ESX-1 knockout strains of the RD1 region show a controversial pattern with regard to phago-lysosomal processing as published by McGurn et al. (Infection and Immunity, 75, 2007). The ESX-1 secretion

deficient ΔeccD1 (putative ESX-1 transmembrane channel) strain was transferred to the lysosome whereas a ΔesxA strain was not. In another study an espL transposon mutant did not arrest phagosomal processing whereas wild-type bacteria did (Brodin et al., PLOSpathogens 2010), however, it is not known whether this mutant is deficient in EsxA secretion. In addition, there are several studies showing that the BCG vaccine strain (deficient in ESX-1 secretion) arrests phagosome maturation, possibly due to up-regulation of compensatory genes. Due to these discrepancies, we decided not to include a mutant strain as a control – furthermore, it is not clear which mutant would have been most appropriate for this experiment. To fully answer the question of ESX-1 dependent arrest in phagosome maturation, these experiments should be performed with a panel of different RD1 and non-RD1 mutants deficient in ESX-1 secretion followed by in-depth analysis of the mechanism behind the different phenotypes - obviously this is far beyond the scope of the present drug screening assay. Interestingly, the ΔphoP mutant (an EsxA secretion mutant) is clearly deficient in blockage of phagosome maturation indicating that sensor kinases impact phagosomal processing of Mtb (Ferrer et al., PLOSone, 2010).

8. While the finding that zinc may be a signal for Esx1 secretion is interesting, the model described in Figure 7 is perhaps beyond the scope of a Resource paper.
We have chosen to retain Figure 7 as it summarizes graphically several important findings.

Edits
1. The labels for Table S1 and Table S3 say RNA-sec, instead of RNA-seq.

This has been changed. Thanks for pointing it out.

2. The figure legend for Figure S3 states: "EsxA and GroEL were detected in the culture filtrate of Mtb Erdman treated with different cell wall biosynthesis inhibitors as well as BBH7 and BTP15". The immunoblot shown here has no visible band for EsxA under BBH7 treatment and a significantly reduce band with BTP15 treatment. This discrepancy should be addressed.

This corresponds to secretion inhibition by these compounds as is also shown in Figure 3 of the manuscript. We improved the legend for Figure S4C (previously Figure S3C) to make this clear.

3. Figure 5a. It would be helpful to label the chemical structure of BTP15.

This has been changed.

4. The manuscript describes the EtBr membrane permeability assays as being Figure 4b when they should be Figure 5b.

This has been changed. Thanks for the correction.

Reviewer #3: The Manuscript by Rybniker et al. is a well written manuscript describing an interesting new screen for novel compounds that alter the virulence of Mycobaterium tuberculosis. The authors take advantage of the observation that Mycobaterium tuberculosis will induce lysis of various cell lines and develop a high throughput screen to identify novel compounds from a 10,000 compound library that inhibit this lysis. They identify a number of interesting hits which they subsequently validate. In an excellent RNA-seq study preformed on Mtb treated with one of the compound they identify which demonstrates that one of these compounds regulates the transcription of the ESX-1 system. In addition they show other compounds attack diverse targets that affect phosphorylation, permeability or membranes bound ATPses. Clearly this is one of the strengths of this paper that it reveals a number of different pathways important for the parthenogenesis and virulence of M. tuberculosis. including a kinase, while other compounds are shown to affect permeability. The authors conclude in the manuscript by saying that these compounds alter phagosome-lysosome fusion maturation for Mtb in macrophages. The work is clearly innovative and provides new tools to study the biology of Mtb. Further studies to asses their roles in animal models would be out of the scope of this original manuscript, but it clear the authors intend to explore these possibilities.

Specific Comments:

1) Line 77 should include a reference to Braunstein et al. 2003. Mol. Microbiol. 48:453-464.

This reference has been inserted.

2) Line 113: the end of the first sentence should include: "as first describes by Hsu et al." (From: Proceedings of the National Academy of Sciences of the United States of America 100, 12420-12425, listed in references)

This suggestion has been adopted as mentioned above in response to Minor Point 1 of reviewer 2.

3) Line 118: Which ΔRD1 mutant are you using in the experiment? Was is made in the Erdman strain or the Mtb strain? Please provide the reference. This is important to know because the screen is done selective of the Erdman strain. I presume this is because the RV strain does not work. Is this true or not? And having the matched isogenic strains could give you different results for this specific experiment.

We agree with reviewer 3 that strain specification is an important issue when investigating and discussing bacterial virulence and we failed to provide these data in the initial submission. The ΔRD1 strain we used in our study is based on the H37Rv genetic background and not on the Erdman strain. To ensure comparability of experiments we included FSA data of the well defined Tn::*pe35 Mtb Erdman transposon mutant in Fig. 1B. This mutant carries a transposon insertion in a promoter upstream of the esxAB genes leading to full abrogation of ESX-1 dependent protein secretion, which is comparable to that seen with ΔRD1 strains (Chen et al. 2013, Mol. Micro. 89:1154-66). In the FSA, this mutant is attenuated*

to the same extent as the H37Rv ΔRD1 strain. This indicates that once ESX-1-dependent protein secretion is fully blocked, the attenuation phenotype in the FSA is high and independent of the genetic background of the original strain used. The ΔespA strain we used in our study is an Erdman strain. The backgrounds of all strains used in this figure are now specified in the materials and methods section (lines 431 - 433).

To comment on the phenotype of the H37Rv strain in the FSA: during setup of the FSA we tested a panel of wild type Mtb strains for efficiency in fibroblast lysis. Though clearly inhibiting fibroblast survival, H37Rv displayed the lowest levels of cytolysis and this correlates well with recent findings of reduced EsxA secretion in H37Rv, which is most likely due to a mutation of the WhiB6 promoter upstream of the RD1 region (Solans et al., Infection and Immunity, 82/8, 2014). This confirms again, that the FSA is a highly sensitive tool to quantify EsxA secretion and justifies our choice of Mtb Erdman for drug screening.

4) Also the strains listed in lines 119 and 120 are neither references in the text nor the figure legends.

Please see the response to point 3 where clarification is now provided.

5) Line 123: Rather than say "all compounds," instead list Isoniazid, Rifampicin, Limezolid, Moxifloxacin, DMSO, Streptomycin, and Kanamycin.

This has been changed on line 117 as suggested.

6) In line 260-273: the zinc regulation of ESXA is a very interesting result. However, is it possible that this is a secondary response to regulation of ESX-3 which then leads to this altered response of ESX-1? Can you please comment?

Recent data suggest a role of ESX-3 in zinc and iron uptake. Key to this was the finding that the ESX-3 system is transcriptionally regulated by the zinc uptake repressor, Zur, and the iron dependent repressor, IdeR (Serafini et al, JB, Vol 191/20, 2009). To our knowledge, there are no data showing that these regulators also affect ESX-1 secretion. Furthermore, as might be expected, ESX-3 responds to low zinc conditions since it seems to be required for zinc uptake, probably due to up-regulation of its substrates, though this has not been shown yet. We observed the opposite for ESX-1 where high zinc levels led to hyper-secretion of EsxA. Thus, it is difficult to identify a link between the divergent responses of ESX-3 and ESX-1 secretion. ESX-1 regulation is complex and several regulatory and sensor proteins have been shown to target ESX-1 promoters. An environmental signal for most of these regulators has not been identified yet and zinc could be one of these signals. Indeed, zinc responsive two-component system such as CzcRS of Pseudomonas aeruginosa are well known regulators of bacterial virulence (Dieppois et al. Plosone 2012 http://www.ncbi.nlm.nih.gov/pubmed/22666466). In our view, the link between zinc, ESX-3 and ESX-1 could be evolutionary. It is possible that an ancestral ESX system was required for heavy metal uptake, and that after gene duplication, one copy diverged into a specialized host modifying ESX-1 system that still responds to zinc concentrations as well as to other stimuli. As a signal to differentiate between extracellular, cytosolic and intraphagosomal localization, responding to zinc levels is physiologically

relevant since these vary widely between these different compartments (Botella et al. 2011, Cell host and microbe 10, 248-259).

*The role of ESX-3 and zinc homeostasis has been explained and cited in the revised version of the manuscript lines 403 – 405: "*Of note, there is evidence that the ESX-3 secretion system is involved in zinc homeostasis of *Mtb* (Serafini et al., 2013). Thus, interference with ESX-3 activity by BBH7 may cause for the zinc stress observed."

See also our response to comment 3 for reviewer 1.

Graphical abstract

Click here to download Graphical Abstract: graphicalabstract.tif

Innovative anti-cytolytic screen identifies potent inhibitors of mycobacterial virulence protein secretion

Jan Rybniker[1,2], Jeffrey M. Chen[1], Claudia Sala[1], Ruben Hartkoorn[1], Anthony Vocat[1], Andrej Benjak[1], Stefanie Boy-Röttger[1], Ming Zhang[1], Rita E. Szekely[1], Zoltán Greff[3], László Örfi[3,4], István Szabadkai[3], János Pató[3], György Kéri[3,5], Stewart T. Cole[1]*

[1] Global Health Institute, Ecole Polytechnique Fédérale de Lausanne (EPFL), CH-1015 Lausanne, Switzerland

[2] 1st Department of Internal Medicine, University of Cologne, D-50937 Cologne, Germany

[3] Vichem Chemie Research Ltd, H-1022 Herman Otto u. 15, Budapest, Hungary

[4] Semmelweis University, Department of Pharmaceutical Chemistry, H-1092, Hőgyes Endre u. 9, Budapest, Hungary

[5] Semmelweis University, Department of Medical Chemistry, Pathobiochemistry and Molecular Biology, H-1094 Tűzoltó u. 37-47, Budapest, Hungary

Running title: Targeting mycobacterial protein secretion

***Corresponding author:**
Prof. Stewart T. Cole
Global Health Institute
Ecole Polytechnique Fédérale de Lausanne (EPFL)
Station 19
CH-1015 Lausanne
Switzerland
E-mail: stewart.cole@epfl.ch
Phone: +41-21-693 1851
Fax: +41-21-693 1790

SUMMARY

***Mycobacterium tuberculosis* (*Mtb*) depends on protein secretion systems like ESX-1 for intracellular survival and virulence. The major virulence determinant and ESX-1-substrate, EsxA, causes tissue damage and necrosis, thereby promoting pathogen spread and dissemination. We developed a fibroblast survival assay (FSA) that exploits this phenotype to select molecules that protect host cells from *Mtb*-induced lysis without being bactericidal *in vitro*. Hit compounds identified in this high-throughput screen blocked secretion of EsxA thus promoting phagosome maturation and substantially reducing bacterial burden in activated macrophages. Target identification studies led to the discovery of BTP15, a benzothiophene inhibitor of the histidine kinase MprB that indirectly regulates ESX-1, and BBH7, a benzyloxybenzylidine hydrazine compound. BBH7 affects metal ion homeostasis in *Mtb* and revealed zinc stress as a signal for EsxA secretion. This novel screening approach extends the target spectrum of small molecule libraries and will help to tackle the mounting problem of antibiotic-resistant mycobacteria.**

HIGHLIGHTS

- *Mycobacterium tuberculosis* causes EsxA-dependent host cell lysis
- EsxA secretion can be targeted in high-throughput screens
- Small molecules with diverse mechanisms of action inhibit EsxA secretion
- Small molecule inhibitors abrogate ESX-1-dependent pathogenicity

INTRODUCTION

Tuberculosis, resulting from infection with *Mycobacterium tuberculosis* (*Mtb*), is a serious global health problem accounting for 1.4 million deaths in 2011 (Lechartier et al., 2014). A major reason for the high morbidity and mortality caused by *Mtb* is the long duration of therapy and increasing multidrug-resistance. Alternative therapeutic agents are needed to combat drug resistance. By screening compounds *in vitro* for growth inhibition of *Mtb*, some progress has been made towards clinically implementing bioactive molecules with new mechanisms of action (Lechartier et al., 2014). However, given the high attrition rate of lead compounds in preclinical and clinical development, alternative screening approaches are needed. Traditional *Mtb* whole cell screens often identify different inhibitors, with the same mechanism of action, of promiscuous targets, a problem that may be solved by more sophisticated phenotypic screens (Lechartier et al., 2014).

Targeting virulence protein secretion can extend the spectrum of existing antibacterial libraries (Feltcher et al., 2010). This radically different approach has been applied to the type III secretion systems (T3SS) of Gram-negative bacteria (Baron, 2010), which inject virulence determinants into eukaryotic cells. Several structurally unrelated molecules block T3SS protein secretion leading to attenuation and bacterial clearance by the immune system (Izore et al., 2011).

Mtb has two essential protein export systems that process most of the secretome: the general secretory (Sec) and twin-arginine pathways (Tat), (Braunstein et al., 2003). Five specialized ESX or type VII secretion systems export protein subsets such as virulence determinants (Feltcher et al., 2010). Among these, ESX-1 is a major, well-

studied virulence protein secretion apparatus comprising several transmembrane proteins, ATPases and essential accessory proteins. Additionally, there are several key regulatory proteins that co-regulate ESX-1 secretion. Various ESX-1-dependent substrates are essential for host-cell invasion, intracellular replication and inhibition of phagosome maturation (MacGurn and Cox, 2007; Stoop et al., 2012). The best understood ESX-1 substrate, EsxA, a 6 kDa protein, is capable of lysing cell membranes leading to cytosolic escape and subsequent dissemination of *Mtb* (De Leon et al., 2012). Loss of the ESX-1 genetic locus in *Mycobacterium bovis* accounts for attenuation of the BCG vaccine (Pym et al., 2002).

The regulatory and core proteins of the ESX-1 and house-keeping secretion systems comprise a multitude of interesting and thus far unexploited drug targets (Chen et al., 2010; Feltcher et al., 2010). ESX-1 cannot be targeted by conventional whole cell screens since it is not essential for bacterial viability *in vitro*. However, target-based screens have largely failed to provide compounds with reasonable activity on *Mtb* (Lechartier et al., 2014).

Here, we developed a robust, whole cell-based high-throughput screen (HTS) broad enough to target essentially all structural and regulatory ESX-1-components yet specific enough to exclude weak compounds. The screen exploited the EsxA-dependent cytolytic activity of *Mtb* and uncovered small molecules that promote survival of *Mtb*-infected human lung fibroblasts by inhibiting ESX-1-dependent protein secretion. The transcriptomic signatures of the most potent hits indicate functions beyond ESX-1 inhibition including cell membrane transport, metal ion homeostasis and signal transduction.

RESULTS

Development of a lung fibroblast based HTS to identify protein secretion inhibitors

To screen small molecule libraries for inhibitors of mycobacterial protein secretion we exploited the cytotoxicity of *Mtb* for eukaryotic cells at high multiplicities of infection (MOI) as first described by Hsu et al. and Takii et al. (Hsu et al., 2003; Takii et al., 2002). As proof of principle, MRC-5 lung fibroblasts were infected with the wild-type Erdman strain and well-defined attenuated mutants deficient in ESX-1 secretion followed by quantification of metabolic activity in fibroblasts (Figure 1A). Wild-type *Mtb* was highly cytotoxic, markedly decreasing fluorescence compared to uninfected cells in this fibroblast survival assay (FSA; Figure 1B). The ΔRD1 mutant, lacking core-genes in the ESX-1 locus, as well as the Tn::*pe35* mutant that does not produce EsxA due to an upstream transposon insertion, failed to lyse MRC-5 fibroblasts. Furthermore, infection with a deletion-mutant of the PhoPR two-component regulatory system or a Δ*espA* mutant led to significantly less cytotoxicity due to impaired EsxA secretion (Figure 1B) (Chen et al., 2013; Gonzalo-Asensio et al., 2008).

We also tested several compounds with known antimycobacterial activity for their ability to protect MRC-5 cells from *Mtb*-induced cell death. As expected, drugs with intracellular activity (rifampicin, isoniazid, linezolid and moxifloxacin) were highly protective whereas aminoglycosides (streptomycin; kanamycin), which fail to penetrate MRC-5 cells, were not (Figure 1C). Since the assay endpoint is survival of eukaryotic cells, we tested host-modifying drugs that have been shown to reduce intracellular bacterial load by inhibiting host kinases such as BCR-Abl, Akt or the secreted

mycobacterial kinase PknG (Lechartier et al., 2014). None of these compounds protected fibroblasts from *Mtb*-induced host cell lysis (Figure S1A). Reducing the MOI led to a minor protective effect of some kinase inhibitors (Figure S1A) indicating that their inactivity in the FSA is primarily due to the choice of cell: fibroblasts versus macrophages.

The FSA was adapted for 384-well plates giving a Z'-factor > 0.5 with rifampicin and DMSO as controls (Figure S1B). To distinguish between anti-virulence compounds and growth inhibitory drugs, all compounds were counter-screened against *Mtb* in the resazurin reduction microtiter assay (REMA). A putative protein secretion inhibitor was defined as a hit compound that protected fibroblasts from *Mtb*-induced cell death in the FSA without affecting bacterial growth in the REMA (Figure 1D).

Outcome of the primary and confirmatory screens

A proprietary library of 10,880 synthetic compounds was screened at a concentration of 5 µM leading to the identification of 450 compounds that inhibited mycobacterial growth in the REMA (Figure 2A). 137 compounds were protective in the FSA, 46 compounds were active in both assays indicating that only 10% of the REMA hit compounds had intracellular activity and were non-cytotoxic for fibroblasts. After a confirmatory screen, 55 of the 91 compounds, which impacted virulence without affecting mycobacterial growth in the primary screen, were validated as true hits (Figure 2A). Cheminformatic analysis identified 6 clusters and 9 singletons. Figure 2B correlates the potency of these hits to the controls and displays the three most abundant core structures. Of note, several analogs of the benzyloxybenzylidene-hydrazines and the benzothiophenes were almost as efficient as rifampicin in protecting fibroblasts from *Mtb*-induced cell-death.

For further studies, we selected a benzyloxybenzylidene-hydrazine compound (BBH7) and a benzothiophene compound (BTP15; Figure S2A) with particularly good FSA activity and a favorable cytotoxicity profile. Both compounds protected fibroblasts in a dose-dependent manner (Figure 2C) with an IC_{50} of 2.4 µM for BBH7 and 1.2 µM for BTP15, while no growth inhibition of *Mtb* was observed *in vitro* at 25 µM concentration (Figure S2B). The MIC_{99} for several other mycobacteria and bacterial pathogens was >100 µM for both compounds (Figure S2C). Intracellular anti-mycobacterial activity was determined by quantifying *Mtb* expressing GFP in infected fibroblasts and here the compounds behaved divergently. BTP15-treated bacteria showed GFP fluorescence comparable to the untreated control whereas no fluorescence was detected in the BBH7 and rifampicin-treated samples (Figure 2D). These data demonstrate that BTP15 did not affect bacterial viability in the FSA, yet was highly protective for fibroblasts exposed to *Mtb,* whereas BBH7 is a potent inhibitor of intracellular growth.

BBH7 and BTP15 inhibit mycobacterial protein secretion at nanomolar concentrations

The main aim of the FSA is to identify potential inhibitors of ESX-1. We exposed *Mtb* cultures to the compounds, harvested the culture filtrates and quantified EsxA by immunoblotting. Intriguingly, both compounds showed dose-dependent secretion inhibition of this major virulence protein (Figure 3). We also quantified Ag85 complex proteins, since these are Tat-dependent substrates. At 5 µM, BBH7 fully blocked Ag85 secretion. For BTP15 we observed a different pattern as, at concentrations ≤10 µM, Ag85 secretion was only slightly affected at best. However, 20 µM BTP15 reduced Ag85 secretion and blocked EsxA secretion fully (Figure 3).

BTP15 deregulates genes controlled by two-component regulatory systems

RNA-seq experiments with compound-treated *Mtb* provided mechanistic insight from specific transcriptomic signatures . Only 35 genes were differentially regulated when *Mtb* was exposed to 5 µM of BTP15 (Table S1). Surprisingly, all 18 significantly down-regulated genes were in the DosR (DevR) regulon (Table S1, Figure 4A). This hypoxia-induced regulon requires the two-component response regulator DosRS, which enables the bacteria to enter a “dormant” non-replicative state ensuring long-term intracellular survival and latency (Park et al., 2003).

In *Mtb* the response regulators PhoPR and MprAB are known to link the DosR-regulon and transcriptional regulation of the ESX-1 secretion system *via* the distal *espACD* locus (Gonzalo-Asensio et al., 2008; Pang et al., 2013; Pang et al., 2007). Deletion of *mprAB* leads to upregulation of *espA* and reduced EsxA secretion (Pang et al., 2013). In the primary RNA-seq experiment *espA* was up-regulated below the threshold of 2 but on analysis by qRT-PCR, *espA* was among the genes with >2 fold differential regulation (Figure. 4A). Thus, reduced EsxA secretion and the subsequent loss of virulence observed could be caused by deregulation of the *espACD* locus. We then quantified transcription levels of the regulatory genes *dosR*, *phoP* and *mprA* after exposure to BTP15. Interestingly, *mprA* expression was significantly down-regulated after 24 and 48 h of treatment (Figure 4B). BTP15 (10 µM) also decreased *mprB* transcript levels 3-fold after 48 h exposure (Figure S3A). Since there is considerable overlap among DosR- and MprA-regulated genes, we compared the BTP15 RNA-seq transcript analysis with published gene expression data on *mprAB* deletion mutants and found that the majority of the 35 deregulated genes (highlighted in Table S1) were also

differentially regulated in this mutant under different conditions (He et al., 2006; Pang et al., 2007).

BTP15 is a kinase inhibitor that inhibits MprB autophosphorylation *in vitro*

Having found that treatment of *Mtb* with BTP15 leads to deregulation of genes controlled by two-component regulatory systems, notably MprAB, we reasoned that the compound might directly affect ATP-dependent signal transducing histidine kinases. Studying histidine phosphorylation is extremely challenging due to the chemical instability of this posttranscriptional modification (Kee and Muir, 2012). An MprB autophosphorylation assay was established using purified truncated MprB as described (Zahrt et al., 2003). Relatively large amounts of MprB (25 µM) were needed to detect the MprB phosphohistidine (Figure 4C), as is common for histidine kinase phosphorylation assays (Saini and Tyagi, 2005). Nonetheless, we demonstrated dose-dependent inhibition of MprB auto-phosphorylation by BTP15 (Figure 4D) but could not accurately determine the IC_{50} value due to the large amount of enzyme used. The non-hydrolyzable ATP analog AMP-PNP can be employed to estimate the potency and specificity of histidine kinase inhibitors having high *in vitro* IC_{50} values (Gilmour et al., 2005). When 10 mM AMP-PNP (34x the *in vitro* IC_{50} of BTP15) was used only incomplete reduction of the phosphohistidine signal was seen whereas 1 mM AMP-PNP had no effect on auto-phosphorylation (Figure 4D) indicating that BTP15 is a much stronger inhibitor of MprB auto-phosphorylation than the ATP-analog.

BBH7 has a pleiotropic inhibitory effect on mycobacterial protein secretion

By immunoblotting, BBH7 was found to impact two different protein secretion systems at concentrations ≤ 5 µM (Figure 3); we also observed a 50% reduction of total culture

filtrate protein when bacteria were exposed to 5 µM BBH7 (not shown). To appreciate its full impact on protein secretion we characterized and quantified the secretome of treated and untreated bacteria by LC/MS-MS. These data confirmed the inhibitory effect of BBH7 on the ESX-1 secretion system (Table S2). In addition, several substrates of the ESX-5 secretion system such as EsxN, EsxM, PE25 and PPE41 were significantly reduced in abundance upon treatment. Reduced secretion of virulence-associated proteins of unknown export mechanism was uncovered showing that BBH7 affects several independent lines of *Mtb* pathogenicity (Table S2).

BBH7 deregulates several transmembrane ATPases and alters mycobacterial cell wall permeability

Since BBH7 substantially impacted mycobacterial protein secretion, we expected major changes in the *Mtb* transcriptome after treatment. Indeed, RNA-seq experiments revealed 144 differentially regulated genes (≥ 2-fold) upon exposure to BBH7. Of these, 121 were up-regulated and the gene expression signature mirrors changes primarily associated with cell wall processes and transport (Figure 5A, Table S3, Figure S4). We found positive regulation of the ESX transmembrane ATPase genes, *eccCa1/eccCb1* and *eccA5/eccE5,* in response to altered ESX-1 and ESX-5-dependent protein secretion. In addition, strong up-regulation of the P-type ATPase genes, *ctpC* and *ctpG,* indicated disturbed cell membrane/cell wall transport not only for secreted proteins but also for ions such as zinc and copper. Several other signs for metal-ion overload were observed: strong up-regulation of the metallothionein *mymT,* the multicopper oxidase *mmcO*, the copper-dependent regulator *ricR* and the RicR-regulated gene *lpqS,* as well as deregulation of the zinc stress responsive genes *cadI*, *rv1993*, *cysK2, esxG and esxH*

(Figure 4A, Table S3) (Botella et al., 2011; Serafini et al., 2013). Indirect targets for metal-ion toxicity are Fe-S proteins, explaining the up-regulation of the Fe-S cluster biogenesis operon SUF (*rv1462–rv1466*), and DNA damage leading to a LexA-driven transcriptional response (Rowland and Niederweis, 2012).

To investigate whether BBH7 alters mycobacterial outer membrane permeability, which might explain the transcriptomic pattern associated with metal-ion toxicity, we performed ethidium bromide (EtBr) uptake assays after treatment with the compounds of interest. Indeed, BBH7-treatment was found to increase EtBr accumulation and fluorescence, a sign of perturbed membrane permeability (Figure 5B). This was not observed with BTP15. Interestingly, BBH7 concentrations as high as 25 µM had no impact on the activity of first- and second-line TB drugs (Figure S5).

Zinc stress augments EsxA secretion

Having established that BBH7 treatment leads to transcriptional signs of zinc and copper stress, we surmised that intracellular metal-ion stress might be the link to inhibition of mycobacterial protein secretion. Thus, we stressed *Mtb* with physiological concentrations of zinc or copper, as encountered in the phagosome, and determined EsxA secretion levels. Surprisingly, growing cells in media containing elevated levels of $ZnSO_4$ led to a significant and dose-dependent increase of EsxA secretion whereas Ag85 secretion remained unchanged (Figure 5C). In the presence of 500 µM zinc, a concentration measured in *Mtb*-infected macrophages (Botella et al., 2011), a six-fold increase in EsxA secretion was observed (Figure 5C, lower panel). Elevated concentrations of copper had no effect on EsxA secretion. These findings indicate that BBH7 does not alter mycobacterial protein secretion by zinc or copper intoxication.

Furthermore, for the first time, we report an environmental signal (elevated zinc levels) that augments EsxA secretion.

Since bacterial transport mechanisms depend on the proton motive force, which is linked to intracellular ATP-levels, the intracellular ATP concentration was measured after BBH7 treatment. Unlike treatment with the ATP-synthase inhibitor bedaquiline (BDQ), ATP levels were not reduced by BBH7 (Figure 5D). To further distinguish BBH7 from well-known, mycobacterial cell wall inhibitors, we investigated whether such compounds affect EsxA secretion. Isoniazid and ethambutol, as well as the thiourea compounds ethionamide and thiacetazone, had no effect on EsxA secretion at 0.5 x MIC (Figure S4C). At 5 x MIC, detection of the cytosolic heat-shock protein GroEL in the culture filtrate indicated cell lysis, which was not observed after BBH7 and BTP15 treatment.

Taken together, these results indicate a novel mechanism of action for BBH7, which alters cell-wall permeability for both export of proteins and import of small molecules, leading to strong up-regulation of genes associated with metal ion overload. However, blockage of EsxA secretion by BBH7 does not seem to be caused by zinc/copper intoxication or ATP-depletion.

BBH7 and BTP15 reduce intracellular bacterial load and promote phagolysosomal fusion in *Mtb*-infected THP-1 macrophages

Using GFP-expressing *Mtb* we had shown that BBH7 strongly affects viability of intracellular bacteria in MRC-5 fibroblasts whereas BTP15 does not (Figure 2D). Since the role of fibroblasts in *in vivo* infections is not clear, we also investigated the activity of

the compounds by infecting activated THP-1 macrophages and quantifying both surviving macrophages and intracellular fluorescent mycobacteria. Treatment with BBH7 and BTP15 protected THP-1 cells from *Mtb*-induced cell death (Figure 6A) and greatly reduced the intracellular bacterial load (Figure 6B, C). Since the ESX-1 secretion system plays a decisive role in the arrest of phagosome maturation in *Mtb*-infected macrophages (MacGurn and Cox, 2007) we investigated whether BBH7 and BTP15 can reverse this phenotype. Activated THP-1 macrophages were infected at an MOI of 0.5 with *Mtb* expressing GFP and treated for 7 days. Subsequently, acidic compartments were stained with Lysotracker Red and co-localization of the dye with fluorescent mycobacteria quantified by confocal microscopy. Treated bacteria were found in acidic compartments at significantly higher levels than untreated bacteria (Figure 6D, E) indicating that reduction of intracellular bacterial load in macrophages is primarily achieved through inhibition of *Mtb*-induced phagosome maturation arrest.

DISCUSSION

In this investigation, we developed and validated a novel phenotypic drug screen based on ESX-1 secretion dependent cytotoxicity of *Mtb*. A HTS of >10,000 small molecules identified two series of compounds that significantly reduced secretion of EsxA at nanomolar concentrations without affecting mycobacterial growth *in vitro,* the benzothiophenes and benzyloxybenzylidine hydrazines. In addition, less potent hit compounds derived from the indoline-2-one core structure as well as several other compounds also impacted ESX-1 function (not shown). This indicates that by selecting

for hits that abrogate cytotoxicity of *Mtb*, the chance of finding inhibitors of ESX-1-dependent protein secretion is relatively high. The reason for this may lie in the nature of the screen itself; *Mtb*-induced host cell lysis at high MOI is almost exclusively associated with secretion of EsxA. Screening deep transposon libraries for mutants with impaired cytolytic activity primarily detected insertions in genes required for EsxA secretion thus highlighting the importance of this virulence determinant (Gao et al., 2004; Hsu et al., 2003). Another key factor for selectivity of the bioassay is our choice of lung fibroblasts for the quantification of *Mtb*-induced cell death. These non-professional phagocytes fail to detect host modifying agents that reduce the intracellular burden of *Mtb* in macrophages (Lechartier et al., 2014). This feature may be beneficial for target identification of these anti-virulence drugs.

The benzothiophene BTP15 is a kinase inhibitor that affects EsxA secretion most likely by deregulating the *espACD* operon. Several transcriptional regulators control ESX-1-dependent secretion by binding to this operon that is not part of the ESX-1 region but nonetheless encodes EsxA co-secreted proteins (Blasco et al., 2012; Gonzalo-Asensio et al., 2008; Pang et al., 2013). An *mprAB* mutant displayed up-regulation of *espA* and greatly reduced EsxA secretion (Pang et al., 2013). Furthermore, MprA co-regulates several DosR-regulated genes and SigE (Pang et al., 2007). BTP15 treatment deregulates a similar set of genes and inhibits MprB auto-phosphorylation *in vitro*. Thus, the two component regulatory system MprAB is the probable BTP-15 target. MprAB is clearly associated with virulence since the corresponding mutants show impaired survival *in vivo*, particularly during the chronic stage of infection (Zahrt and Deretic, 2001). Macrophages infected with a Δ*mprAB* strain elicit significantly lower levels of

tumor necrosis factor alpha and interleukin 1β similar to *Mtb* strains deleted for *espACD* or the ESX-1 region (Pang et al., 2013). MprAB also seems to regulate the ESX-1 region itself since the *mprAB* mutant fails to secrete EspB, a protein that is not influenced by the *espACD* operon (Chen et al., 2013; Pang et al., 2013). We also found inhibition of EspB secretion upon BTP15 treatment (Figure S3B), accompanied by greater attenuation than seen with a Δ*espA* mutant in the FSA. However, in contrast to BTP15-treated macrophages, which show reduced intracellular bacterial load, loss of *mprAB* does not reduce the number of intracellular bacteria in activated macrophages (Zahrt and Deretic, 2001). Low expression levels of *dosR*, *phoP* and *mprA* were revealed by qRT-PCR experiments although subtle transcriptional changes during drug treatment may not have been detected. Many of the ESX-1 regulatory genes are induced during intracellular infection, thus BTP15 may have an extended impact on virulence gene expression inside macrophages and fibroblasts explaining the discrepancy between the intracellular behavior of the Δ*mprAB* mutant and BTP15-treated bacteria.

Bacterial histidine sensor kinases and two component regulatory systems are indeed interesting drug targets. Potent inhibitors with good *in vivo* activity have been generated for Gram-negative pathogens (Rasko et al., 2008). Deletions of these regulatory genes often cause severe attenuation as illustrated impressively by the *Mtb* Δ*phoPR* mutant, which is currently being developed as a live TB vaccine (Gonzalo-Asensio et al., 2008). Histidine kinase domains are structurally distinct from eukaryotic serine, threonine and tyrosine kinases and this may enable kinase inhibitors with selective antibacterial activity to be developed (Kee and Muir, 2012). However, unlike serine, threonine and tyrosine kinases, where a plethora of *in vitro* and *in vivo* tools are

available, histidine kinase research is handicapped by a lack of biochemical tools, largely due to the chemical instability of this posttranslational modification (Kee and Muir, 2012). Nevertheless, with the FSA we provide a validated assay for targeting membrane-bound kinases and other ESX-1 regulatory proteins with small molecules.

While there is considerable knowledge of the proteins involved in transmembrane export of substrates nothing is known of the fate of proteins once translocated to the periplasm nor of the mechanism for export through the mycomembrane. Again, putative pore and channel proteins involved in these processes may be interesting drug targets due to their extracytoplasmic location, which may facilitate drug accessibility. This notion is supported by the discovery of a broad spectrum inhibitor of three unrelated secretion systems in Gram-negative pathogens that is believed to target outer-membrane pore proteins shared by several translocation systems (Felise et al., 2008). With BBH7 we identified a pleiotropic inhibitor of mycobacterial protein secretion. However, the gene expression signature following exposure to BBH7, with strong up-regulation of several P-type ATPases as well as altered EtBr uptake in treated bacteria, suggests disturbed export not only for proteins but also for smaller molecules. This makes a common pore structure exclusively dedicated to protein transport through the cell envelope an unlikely target of BBH7. Rather, it is conceivable that this compound has a more general impact on processes involved in cell wall biogenesis.

Another possible mechanism of action for BBH7 is depletion of the ATP source for the membrane-bound transport ATPases that is linked to the proton-motive force. Although some protonophores also inhibit bacterial protein translocation, we provide several independent datasets that functionally separate BBH7. First, protonophores are

known to deplete the intracellular ATP-pool of *Mtb* rapidly (Boshoff et al., 2004), which was not the case for treatment with BBH7. Second, the transcriptional signature of protonophore compounds, with strong up-regulation of the *cyd*-operon and genes of the respiratory chain (Boshoff et al., 2004), is distinct from the BBH7 response. Third, unlike BBH7, the non-selective protonophores are highly cytotoxic for *Mtb* (Brown and Parish, 2008) as well as for eukaryotic cells.

There are distinct signs of zinc and copper stress in bacteria exposed to BBH7. Intra-phagosomal zinc/copper accumulation as a means for host defense has emerged as an exciting field in mycobacterial research (Botella et al., 2011; Rowland and Niederweis, 2012). In this context, our finding of zinc-enhanced secretion of EsxA might represent a novel mycobacterial defense mechanism to counteract heavy metal toxicity. Until now, no environmental signal that induces secretion of EsxA was known. We propose a model where, after phagocytosis, the cation exporters, CtpC and CtpG, are up-regulated to rapidly relieve cytosolic zinc stress (Figure 7A). However, the phagosome is a closed environment so the initial up-regulation of P-type-ATPases will reduce zinc-levels in the bacterial cytosol but not in the phagosome. More sustained alleviation of metal-ion stress may be *via* EsxA-mediated lysis of the phagosomal membrane (Figure 7A). In fact, EsxA-dependent leakage of potassium ions and efflux of charged fluorophores from phagosomal membranes was recently reported (De Leon et al., 2012). Pore-forming toxin-dependent ion efflux from the phagosome or the host cell membrane is a hallmark of most intracellular bacterial pathogens (Gonzalez et al., 2008).

This model also implies a dual and probably synergistic effect of BBH7 on mycobacterial virulence. BBH7 increases outer membrane permeability and leads to heavy metal stress. The bacterium responds by up-regulating the EsxA-translocating ATPases EccCb1 and EccCa1, however, EsxA secretion is blocked by BBH7, which leaves the phagosomal membrane intact and possibly leads to further accumulation of toxic substances in the phagosome (Figure 7B). This mechanism may explain the high rate of phagocytosed bacteria co-localizing with lysosomes and the potent intracellular growth inhibition we observed in BBH7-treated macrophages and fibroblasts. Of note, there is evidence that the ESX-3 secretion system is involved in zinc homeostasis of *Mtb* (Serafini et al., 2013). Thus, interference with ESX-3 activity by BBH7 may cause for the zinc stress observed.

The molecules identified in this work would have escaped detection by conventional whole cell screens. By selecting for a specific phenotype strongly associated with mycobacterial virulence, the hit-spectrum of a given library can be extended as demonstrated here. Also, we show that molecules protecting eukaryotic cells from *Mtb*-induced cytotoxicity may affect mycobacterial virulence beyond EsxA secretion (dormancy, small molecule influx). The data indicate that anti-virulence drugs are capable of reducing the intracellular bacterial load by inducing phagosomal processing in professional phagocytes at levels similar to first-line drugs (Ramachandra et al., 2005).

Our assay format provides both a rapid readout and information about the bactericidality, anti-virulence effect, cytotoxicity and intracellular activity of the hits. Screening novel compound libraries or rescreening existing collections using the FSA

may identify additional hits, with novel mechanisms of action, for lead optimization. Furthermore, compounds from other intracellular screens showing a discrepancy between intracellular IC_{50} and MIC in broth should be tested for inhibition of EsxA secretion, which may facilitate identification of their targets. Finally, our robust screening strategy based on inhibition of pathogen driven host-cell toxicity could also be adopted for anti-virulence drug screens targeting toxin-secreting bacteria such as *Clostridium difficile* where alternative treatment approaches are urgently needed.

EXPERIMENTAL PROCEDURES

Bacterial culture conditions and eukaryotic cell lines

Full description of experimental procedures and reagents used can be found in the supplemental information. Mycobacterial strains were routinely grown in Middlebrook 7H9 broth (supplemented with 0.2% glycerol, 10% ADC and 0.05% Tween-80) or in Sauton's medium for culture filtrate analysis. ESX-1 mutants used for proof of principle studies were H37Rv-ΔRD1, *Mtb*-Erdman Tn::*pe35*, *Mtb*-Erdman-Δ*espA* (Chen et al., 2013) and *Mtb*-MT103 *ΔphoP* (Gonzalo-Asensio et al., 2008). MRC-5 human lung fibroblasts, from the Corriell Institute for Medical Research, were grown in MEM-medium supplemented with 10% heat inactivated fetal bovine serum (FBS), 1% non-essential amino acids and 1 mM sodium pyruvate. THP-1 macrophages were grown in RPMI-medium supplemented with 10% FBS. Both cell lines were grown at 37°C with 5% CO_2.

HTS

Library compounds were preplated into cellbind 384-well microplates (Corning) at a concentration of 50 µM in 5 µl of 5% DMSO. MRC-5 cells grown to late log phase were harvested and seeded at 4,000 cells/well in a volume of 35 µl using an automated microplate dispenser (multidrop combi, Thermo Scientific). Cells were allowed to adhere for 3 h before washed, mid-logarithmic phase *Mtb*-Erdman cells were added to the assay plates at an MOI of 10 in 10 µl of MEM medium. Plates were sealed and incubated at 37°C under 5% CO_2. Rifampicin (5 µg/ml) was used as a control, see Figure 1 for assay plate layout. After 72 h, plates were left at room temperature (RT) for 1 h and 5 µl of Prestoblue cell viability reagent (Life Technologies) added. After 1 h at RT, fluorescence was measured in a Tecan infinite M200 plate reader (excitation 570 nm, emission 590 nm; fluorescence generated by the bacteria was negligible). REMA assays were performed in 7H9 broth using a starting OD of 0.0001, a 7 day incubation period and a final volume of 10% resazurin (0.025% w/v). Z'-factor determinations were as described in the supplemental information. Replicates were considered as hits if their values were superior to the mean of the negative control values plus 3 standard deviations. The final score was the mean value of the replicates.

Immunoblots and secretome analysis

Protein preparation and immunoblots were performed as described recently (Chen et al., 2013). In brief, 30 ml of bacteria grown to mid-logarithmic phase (OD_{600} of 0.6 to 0.7) in Sauton's medium supplemented with 0.05% Tween 80 were centrifuged and resuspended in Sauton's medium without Tween. Compounds were added at concentrations as indicated and cells were grown further at 37°C with shaking for 4

days. Cultures were harvested by centrifugation to obtain culture filtrates and cell pellets. Culture filtrates were concentrated 100-fold in 5-kDa cutoff Vivaspin columns (Sartorius). Cell lysates were prepared by bead beating bacterial pellets in lysis buffer with 100-µm glass beads.

For immunobloting, 5 µg of protein were resolved by SDS-PAGE and transferred to nitrocellulose membranes. Membranes were blocked with TBS-buffer (3% milk powder) and incubated overnight with the desired primary antibody diluted in TNT-buffer supplemented with 1% BSA fraction V. Membranes were washed with TNT, incubated with the appropriate secondary antibody in TNT-BSA, washed again with TNT, and developed. GroEL2 was used as lysis control for culture filtrates and loading control for cell lysates.

Protein preparation for secretome analysis, dimethyl-labeling and mass spectrometric analysis were performed as described in the supplementary methods.

RNA extraction, qRT-PCR and RNA-seq

For transcriptomics, bacteria were grown under the same conditions as for protein secretion assays. Drug exposure was 8 h at 5 µM for RNA-seq experiments and confirmatory qRT-PCR. RNA was extracted with Trizol (Invitrogen) and treated with DNase I (Roche) prior to library preparation or generation of the cDNA template. cDNA was synthesized using the RevertAid First Strand cDNA Synthesis Kit (Fermentas) using random hexamer primers. cDNA corresponding to 10 ng of input RNA was used in each RT-PCR reaction supplemented with specific primer pairs (200 nM each) listed in Table S4 and SYBR-Green master mix (Applied Biosystems). Quantitative RT-PCR reactions

were performed with the 7900HT Fast Real-Time PCR System (Applied Biosystems) as follows: 50°C for 2 min, 95°C for 10 min, then 40 cycles of 95°C for 15 s and 60°C for 60 s. Melt curve analysis confirmed specific amplification for each primer pair.

For the RNA-seq library preparation 100 ng of total RNA were used in the TruSeq Stranded mRNA LT kit, according to the instructions provided by Illumina. An aliquot was analyzed on Qubit and Fragment Analyzer prior to sequencing on an Illumina HiSeq using the TruSeq SR Cluster Generation Kit v3 and TruSeq SBS Kit v3. Data were processed with the Illumina Pipeline Software v1.82. RNA-seq data were deposited in the Gene Expression Omnibus (GEO) server at the National Center for Biotechnology Information (NCBI).

Quantification of intracellular ATP-levels and EtBr uptake assays

Bacteria were grown for 24 h with test compounds and the BacTiter-Glo viability reagent (Promega) used to quantify ATP levels as per the manufacturer's recommendations. For EtBr uptake assays, bacteria were washed with PBS containing 0.05 % Tween 80, OD_{600} was adjusted to 0.4 and 100 µl were pipetted into black 96 well plates. EtBr was added (4 µM final concentration) and fluorescence read every 2 min at 545/600 nm.

Fluorescence microscopy

THP-1 macrophages were activated on round 9 mm cover slips in 24 well plates (10^5 cells/well) with 100 nM of phorbol-12-myristate-13-acetate for 72 h. To quantify intracellular *Mtb* Erdman-GFP, macrophages were infected at an MOI of 2 for 12 h. Cells were washed to remove unphagocytosed bacteria and fresh medium containing compounds or DMSO was added. After incubation for four days, cells were washed, fixed with 4% paraformaldehyde/PBS and stained with Dapi-Fluoromount-G

(SouthernBiotech). Images were acquired on a Zeiss LSM 700 using ZEN imaging software and Fiji processing software. At least forty fields of three separate monolayers were collected for image processing and statistical analysis. For intracellular localization studies cells were prepared as described above and infected at an MOI of 0.5. After 12 h, extracellular bacteria were removed by washing with PBS and fresh medium containing compounds or DMSO was added. Incubation continued for a total of 7 days with replacement of media plus compounds after 3 days. Fresh medium containing 50 nM Lysotracker Red (Life Technologies) was added for 2 h. Cells were washed and fixed as described above. Colocalization rates of GFP-fluorescing phagosomes and Lysotracker Red were determined by analyzing >100 phagosomes from at least three separate monolayers.

Protein purification and kinase inhibitor assay

Proteins were purified as described (Rybniker et al., 2014). For autophosphorylation assays, MprB lacking its N-terminal transmembrane domain was incubated with [γ-^{32}P]ATP (10 mCi/ml, 3,000 Ci/mmol) in 50 mM Tris-HCl (pH 7.5), 50 mM KCl and 20 mM $MnCl_2$ for 1 h. Reactions were stopped by heating in SDS-loading buffer for 5 min at 80°C followed by sample separation using SDS-PAGE. Gels were either stained with Coomassie brilliant blue or dried for 2 h at 60°C in a model 583 gel dryer (Biorad) followed by exposure to X-ray film overnight or counting of ^{32}P-incorporation into band equivalents using a LS6500 scintillation counter (Beckman-Coulter). For kinase inhibitor assays, compounds were pre-incubated with MprB for 3 h prior to addition of [γ-^{32}P]ATP.

Statistical analyses

Unpaired Student's T-tests were used throughout.

SUPPLEMENTAL INFORMATION

Supplemental Information includes five figures, three tables, Supplemental Experimental Procedures and References, and may be found on-line with this article.

AUTHOR CONTRIBUTIONS

J.R. and S.T.C. designed the study. J.R., J.M.C., C.S., R.H., A.V., S.B-R., M.Z. and R.E.S. performed biological experiments and analyzed the data. A.B. performed bioinformatics. Z.G., L.O., I.S., J.O. and G.K. designed and synthesized compounds and analyzed chemistry results. J.R. and S.T.C. wrote the paper with input and approval from all authors.

ACKNOWLEDGMENTS

We thank our EPFL colleagues M. Chambon, D. Banfi and N. Ballanfat for help with assay development; D. Chiappe and R. Hamelin for mass spectrometry; T. Laroche and R. Guillet for confocal microscopy; N. Dhar for providing strains; S. Georgeon and O. Hantschel for advice on kinase assays.

This work was supported in part by grants from Vichem and the Swiss National Science Foundation (grant number 31003A_140778). J.R. was supported by the German Federal Ministry of Research and Education (BMBF grant 01KI1017) and R.E.S. by a European Commission Marie Curie Fellowship (PIEF-GA-2012-327219).

G.K. is CEO/CSO and founder of Vichem Chemie Research Ltd; L.Ö. is co-founder, COO & VP of Chemistry; G.K., L.Ö., Z.G., I.S. and J.P. are Vichem employees.

All other authors declare no financial interest.

REFERENCES

Baron, C. (2010). Antivirulence drugs to target bacterial secretion systems. Current opinion in microbiology *13*, 100-105.

Blasco, B., Chen, J.M., Hartkoorn, R., Sala, C., Uplekar, S., Rougemont, J., Pojer, F., and Cole, S.T. (2012). Virulence regulator EspR of Mycobacterium tuberculosis is a nucleoid-associated protein. PLoS pathogens *8*, e1002621.

Boshoff, H.I., Myers, T.G., Copp, B.R., McNeil, M.R., Wilson, M.A., and Barry, C.E., 3rd (2004). The transcriptional responses of Mycobacterium tuberculosis to inhibitors of metabolism: novel insights into drug mechanisms of action. The Journal of biological chemistry *279*, 40174-40184.

Botella, H., Peyron, P., Levillain, F., Poincloux, R., Poquet, Y., Brandli, I., Wang, C., Tailleux, L., Tilleul, S., Charriere, G.M.*, et al.* (2011). Mycobacterial p(1)-type ATPases mediate resistance to zinc poisoning in human macrophages. Cell host & microbe *10*, 248-259.

Braunstein, M., Espinosa, B.J., Chan, J., Belisle, J.T., and Jacobs, W.R., Jr. (2003). SecA2 functions in the secretion of superoxide dismutase A and in the virulence of Mycobacterium tuberculosis. Molecular microbiology *48*, 453-464.

Brown, A.C., and Parish, T. (2008). Dxr is essential in Mycobacterium tuberculosis and fosmidomycin resistance is due to a lack of uptake. BMC microbiology *8*, 78.

Chen, J.M., Pojer, F., Blasco, B., and Cole, S.T. (2010). Towards anti-virulence drugs targeting ESX-1 mediated pathogenesis of Mycobacterium tuberculosis. Drug Discovery Today Disease Mechanisms *01/2010*, e25-e31.

Chen, J.M., Zhang, M., Rybniker, J., Boy-Rottger, S., Dhar, N., Pojer, F., and Cole, S.T. (2013). Mycobacterium tuberculosis EspB binds phospholipids and mediates EsxA-independent virulence. Molecular microbiology *89*, 1154-1166.

De Leon, J., Jiang, G., Ma, Y., Rubin, E., Fortune, S., and Sun, J. (2012). Mycobacterium tuberculosis ESAT-6 exhibits a unique membrane-interacting activity that is not found in its ortholog from non-pathogenic Mycobacterium smegmatis. The Journal of biological chemistry *287*, 44184-44191.

584 Felise, H.B., Nguyen, H.V., Pfuetzner, R.A., Barry, K.C., Jackson, S.R., Blanc, M.P.,
585 Bronstein, P.A., Kline, T., and Miller, S.I. (2008). An inhibitor of gram-negative bacterial
586 virulence protein secretion. Cell host & microbe *4*, 325-336.

587 Feltcher, M.E., Sullivan, J.T., and Braunstein, M. (2010). Protein export systems of
588 Mycobacterium tuberculosis: novel targets for drug development? Future microbiology *5*,
589 1581-1597.

590 Gao, L.Y., Guo, S., McLaughlin, B., Morisaki, H., Engel, J.N., and Brown, E.J. (2004). A
591 mycobacterial virulence gene cluster extending RD1 is required for cytolysis, bacterial
592 spreading and ESAT-6 secretion. Molecular microbiology *53*, 1677-1693.

593 Gilmour, R., Foster, J.E., Sheng, Q., McClain, J.R., Riley, A., Sun, P.M., Ng, W.L., Yan,
594 D., Nicas, T.I., Henry, K.*, et al.* (2005). New class of competitive inhibitor of bacterial
595 histidine kinases. Journal of bacteriology *187*, 8196-8200.

596 Gonzalez, M.R., Bischofberger, M., Pernot, L., van der Goot, F.G., and Freche, B.
597 (2008). Bacterial pore-forming toxins: the (w)hole story? Cell Mol Life Sci *65*, 493-507.

598 Gonzalo-Asensio, J., Mostowy, S., Harders-Westerveen, J., Huygen, K., Hernandez-
599 Pando, R., Thole, J., Behr, M., Gicquel, B., and Martin, C. (2008). PhoP: a missing piece
600 in the intricate puzzle of Mycobacterium tuberculosis virulence. PloS one *3*, e3496.

601 He, H., Hovey, R., Kane, J., Singh, V., and Zahrt, T.C. (2006). MprAB is a stress-
602 responsive two-component system that directly regulates expression of sigma factors
603 SigB and SigE in Mycobacterium tuberculosis. Journal of bacteriology *188*, 2134-2143.

604 Hsu, T., Hingley-Wilson, S.M., Chen, B., Chen, M., Dai, A.Z., Morin, P.M., Marks, C.B.,
605 Padiyar, J., Goulding, C., Gingery, M.*, et al.* (2003). The primary mechanism of
606 attenuation of bacillus Calmette-Guerin is a loss of secreted lytic function required for
607 invasion of lung interstitial tissue. Proceedings of the National Academy of Sciences of
608 the United States of America *100*, 12420-12425.

609 Izore, T., Job, V., and Dessen, A. (2011). Biogenesis, regulation, and targeting of the
610 type III secretion system. Structure *19*, 603-612.

611 Kee, J.M., and Muir, T.W. (2012). Chasing phosphohistidine, an elusive sibling in the
612 phosphoamino acid family. ACS chemical biology *7*, 44-51.

613 Lechartier, B., Rybniker, J., Zumla, A., and Cole, S.T. (2014). Tuberculosis drug
614 discovery in the post-post-genomic era. EMBO Mol Med.

615 MacGurn, J.A., and Cox, J.S. (2007). A genetic screen for Mycobacterium tuberculosis
616 mutants defective for phagosome maturation arrest identifies components of the ESX-1
617 secretion system. Infection and immunity *75*, 2668-2678.

618 Pang, X., Samten, B., Cao, G., Wang, X., Tvinnereim, A.R., Chen, X.L., and Howard,
619 S.T. (2013). MprAB regulates the espA operon in Mycobacterium tuberculosis and
620 modulates ESX-1 function and host cytokine response. Journal of bacteriology *195*, 66-
621 75.

622 Pang, X., Vu, P., Byrd, T.F., Ghanny, S., Soteropoulos, P., Mukamolova, G.V., Wu, S.,
623 Samten, B., and Howard, S.T. (2007). Evidence for complex interactions of stress-
624 associated regulons in an mprAB deletion mutant of Mycobacterium tuberculosis.
625 Microbiology *153*, 1229-1242.

626 Park, H.D., Guinn, K.M., Harrell, M.I., Liao, R., Voskuil, M.I., Tompa, M., Schoolnik,
627 G.K., and Sherman, D.R. (2003). Rv3133c/dosR is a transcription factor that mediates
628 the hypoxic response of Mycobacterium tuberculosis. Molecular microbiology *48*, 833-
629 843.

630 Pym, A.S., Brodin, P., Brosch, R., Huerre, M., and Cole, S.T. (2002). Loss of RD1
631 contributed to the attenuation of the live tuberculosis vaccines Mycobacterium bovis
632 BCG and Mycobacterium microti. Molecular microbiology *46*, 709-717.

633 Ramachandra, L., Smialek, J.L., Shank, S.S., Convery, M., Boom, W.H., and Harding,
634 C.V. (2005). Phagosomal processing of Mycobacterium tuberculosis antigen 85B is
635 modulated independently of mycobacterial viability and phagosome maturation. Infection
636 and immunity *73*, 1097-1105.

637 Rasko, D.A., Moreira, C.G., Li de, R., Reading, N.C., Ritchie, J.M., Waldor, M.K.,
638 Williams, N., Taussig, R., Wei, S., Roth, M*., et al.* (2008). Targeting QseC signaling and
639 virulence for antibiotic development. Science *321*, 1078-1080.

640 Rowland, J.L., and Niederweis, M. (2012). Resistance mechanisms of Mycobacterium
641 tuberculosis against phagosomal copper overload. Tuberculosis (Edinb) *92*, 202-210.

642 Rybniker, J., Pojer, F., Marienhagen, J., Kolly, G.S., Chen, J.M., van Gumpel, E.,
643 Hartmann, P., and Cole, S.T. (2014). The cysteine desulfurase IscS of Mycobacterium
644 tuberculosis is involved in iron-sulfur cluster biogenesis and oxidative stress defense.
645 The Biochemical journal.

646 Saini, D.K., and Tyagi, J.S. (2005). High-throughput microplate phosphorylation assays
647 based on DevR-DevS/Rv2027c 2-component signal transduction pathway to screen for
648 novel antitubercular compounds. J Biomol Screen *10*, 215-224.

649 Serafini, A., Pisu, D., Palu, G., Rodriguez, G.M., and Manganelli, R. (2013). The ESX-3
650 secretion system is necessary for iron and zinc homeostasis in Mycobacterium
651 tuberculosis. PloS one *8*, e78351.

652 Stoop, E.J., Bitter, W., and van der Sar, A.M. (2012). Tubercle bacilli rely on a type VII
653 army for pathogenicity. Trends in microbiology *20*, 477-484.

654 Takii, T., Yamamoto, Y., Chiba, T., Abe, C., Belisle, J.T., Brennan, P.J., and Onozaki, K.
655 (2002). Simple fibroblast-based assay for screening of new antimicrobial drugs against
656 Mycobacterium tuberculosis. Antimicrobial agents and chemotherapy *46*, 2533-2539.

657 Zahrt, T.C., and Deretic, V. (2001). Mycobacterium tuberculosis signal transduction
658 system required for persistent infections. Proceedings of the National Academy of
659 Sciences of the United States of America *98*, 12706-12711.

660 Zahrt, T.C., Wozniak, C., Jones, D., and Trevett, A. (2003). Functional analysis of the
661 Mycobacterium tuberculosis MprAB two-component signal transduction system.
662 Infection and immunity *71*, 6962-6970.

663

664

FIGURE LEGENDS

Figure 1. Principle of fibroblast-based HTS for identification of protein secretion inhibitors

A) Pipetting and incubation scheme of the FSA. For drug screens, compounds were added to empty 384 well plates followed by addition of fibroblasts.

B) Well-defined ESX-1 mutants are deficient in killing fibroblasts (mean values and standard deviation (± SD)).

C) Antimycobacterial compounds with intracellular activity protect fibroblasts from *Mtb*-induced cytotoxicity (10 µM, ± SD).

D) Plate-layout for HTS and identification scheme for putative protein secretion inhibitors. **(See also Figure S1)**

Figure 2. Outcome of primary and confirmatory screens

A) Hit rate of FSA and REMA in primary and confirmatory screens.

B) Potency of 55 FSA hit compounds (5 µM) in comparison to rifampicin (5 µg/ml) and DMSO controls. Core structures of three most abundant scaffolds.

C) BTP15 and BBH7 protect fibroblasts from *Mtb*-induced killing in a dose-dependent manner.

D) BTP15 has no influence on GFP expression by *Mtb* indicating that BTP15 is not bactericidal in fibroblasts (5 µM, ± SD) whereas BBH7 reduces the GFP-signal comparable to rifampicin-treated fibroblasts. **(See also Figure S2)**

Figure 3. BTP15 and BBH7 affect EsxA secretion of *Mtb*

Bacteria were exposed to different concentrations of compound. After four days EsxA, Ag85 and GroEL (cell lysis control), were detected by immunoblotting culture filtrate (CF) and cell lysate (CL).

Figure 4. Kinase inhibitor BTP15 deregulates genes of the MprAB regulon

A) qRT-PCR of BTP15-treated samples. BTP15 leads to down-regulation (>1.5 fold) of DosR/MprAB associated genes and up-regulation (>2 fold) of *espA* (± SD).

B) Transcriptional levels of three two-component regulatory genes followed by qRT-PCR at three different time-points after treatment with two different concentrations. BTP15 down-regulates *mprA* after 24 and 48 h of treatment (± SD).

C) Coomassie blue stained SDS-PAGE of affinity purified MprB and autophosphorylation of MprB after incubation with [γ-^{32}P]ATP detected by autoradiography.

D) 25 µM of MprB were treated with BTP15 and incorporation of ^{32}P was quantified by scintillation counting. BTP15 leads to a dose-dependent inhibition of autophosphorylation. Non-hydrolysable AMP-PNP was used as a control at 1 and 10 mM (±SD). **(See also Figure S3, Table S1)**

Figure 5. BBH7 induces several P-type-ATPases and alters outer membrane permeability

A) Selection of up- and down-regulated genes upon exposure to BBH7 (5 µM).

B) BBH7 treatment (10 µM) leads to increased EtBr uptake indicating altered outer membrane permeability. Representative example of three individual experiments.

C) Addition of zinc strongly induces EsxA secretion in a dose-dependent manner. The Tat-substrate Ag85 is not affected by this treatment. Band intensity of EsxA in the CF was quantified in the lower panel. (CF: culture filtrate, CL: cell lysate; representative example of three individual experiments).

D) BBH7 and BTP15 (10 µM) have no impact on ATP-levels of *Mtb,* the ATP-synthase inhibitor Bedaquiline (BDQ, 60 ng/ml) was used as a control. Relative light units (RLU) were adjusted to OD values (±SD). **(See also Figures S4, S5, Tables S2, S3)**

Figure 6. BTP15 and BBH7 promote phago-lysosomal fusion and reduce bacterial load in activated THP-1 macrophages

A) Survival of activated THP-1 macrophages was quantified as performed with MRC-5 lung fibroblasts. Both compounds (10 µM) protect the cells from *Mtb*-induced cytotoxicity

B/C) *Mtb*-GFP was quantified inside activated THP-1 cells after treatment with BBH7 and BTP15 (10 µM) as described in the methods. Both compounds significantly reduce the intracellular bacterial load. For BTP15 this contrasts with treatment of infected fibroblasts where intracellular replication is not affected (Figure 2D) Scale bar: 100 µm.

D/E) Confocal microscopy of infected THP-1 macrophages after treatment with two compounds (10 µM) or vehicle (DMSO). After 7 days, acidic compartments were stained with Lysotracker Red and co-localization of *Mtb*-GFP with these compartments quantified (Scale bar: 20 µm). Both compounds promote phagolysosomal fusion to higher levels than DMSO-treated bacteria. *P*-values ≤0.001 = ***; ≤0.01 = ** (±SD).

Figure 7. Model for zinc-induced EsxA secretion and implications for BBH7 function

A) After phagocytozing *Mtb* macrophages recruit heavy metal transporting ATPases like ATP7A to the phagosomal membrane leading to intraphagosomal accumulation of toxic amounts of copper and zinc. This triggers a mycobacterial response involving up-regulation of P-type ATPases (CtpC/CtpG) and metal-chelating proteins to clear intracellular copper and zinc. In addition, elevated zinc concentrations induce secretion of EsxA leading to subsequent phagosomal damage and ion-efflux thus providing a second line of defense against host-driven heavy metal intoxication.

B) Treatment with BBH7 alters mycobacterial outer membrane permeability leading to transcriptional signs of copper and zinc stress. CtpC and CtpG will promote heavy metal efflux into the phagosomal vacuole. In parallel, the ESX-1 translocating ATPases EccCa1 and EccCb1 are up-regulated, however, EsxA secretion is blocked probably leading to phagosomal integrity, further heavy metal accumulation in the phagosome and poisoning of *Mtb*.

Figure 1
Click here to download high resolution image

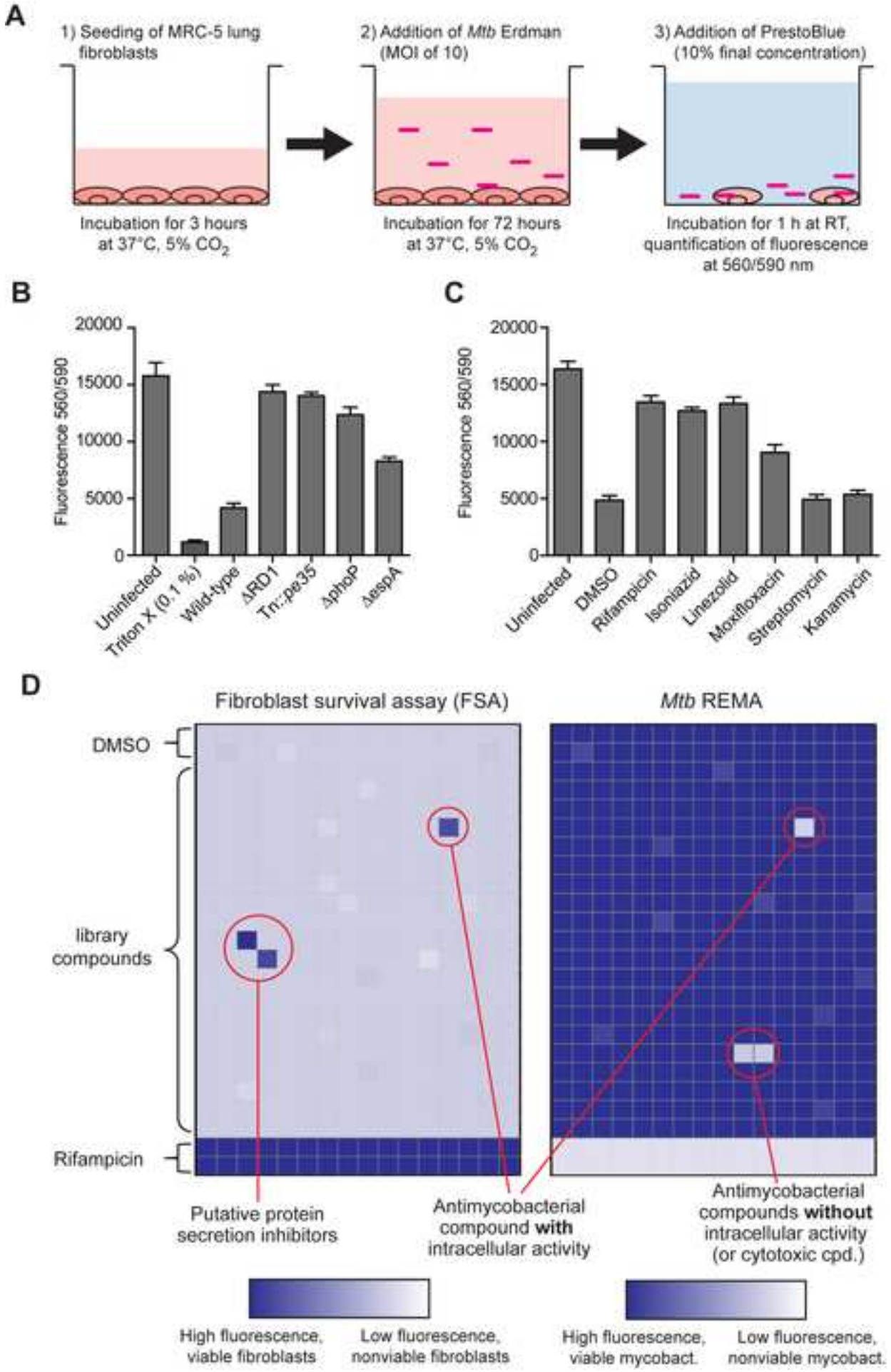

Figure 2
Click here to download high resolution image

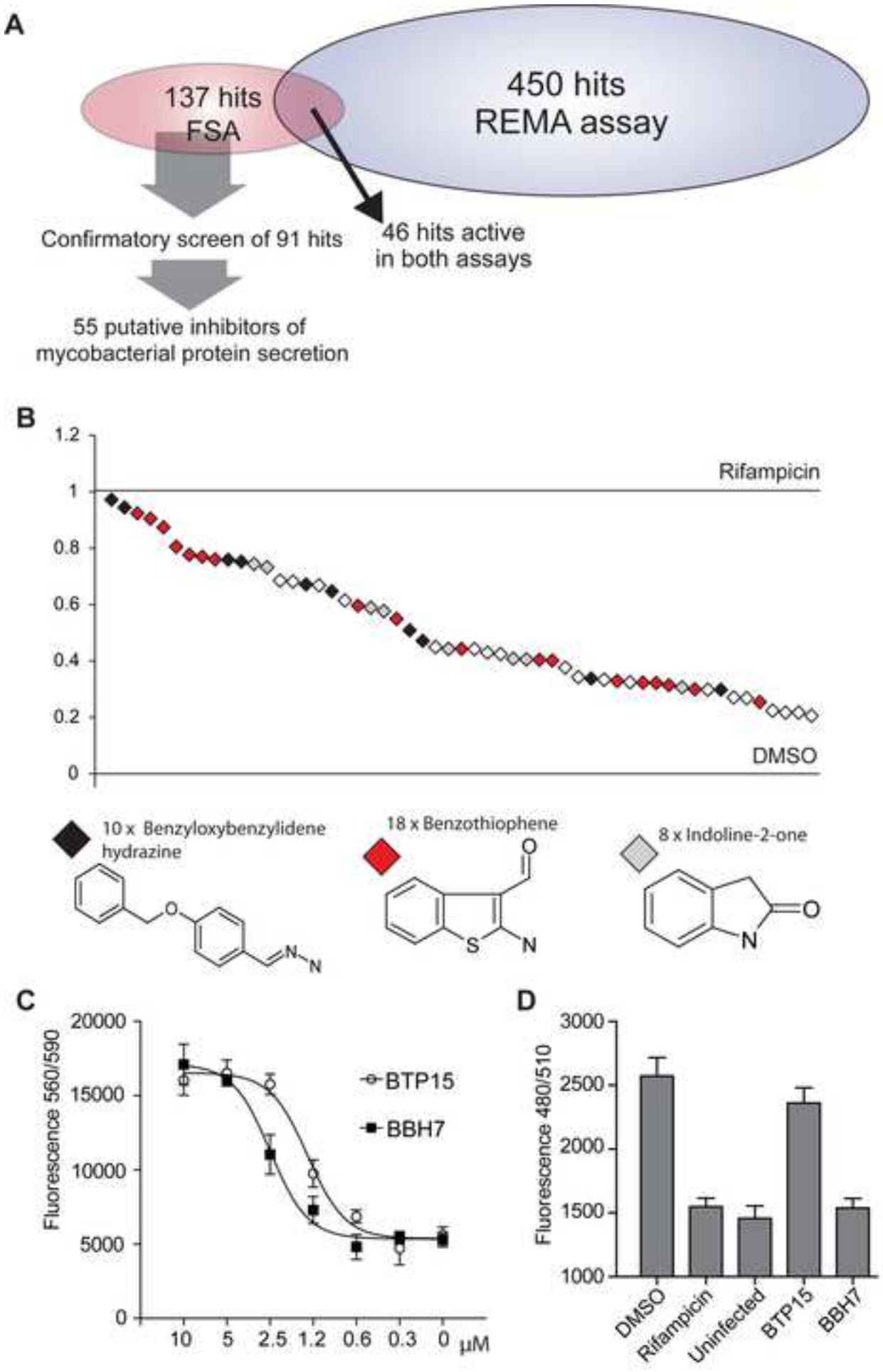

Figure 3
Click here to download high resolution image

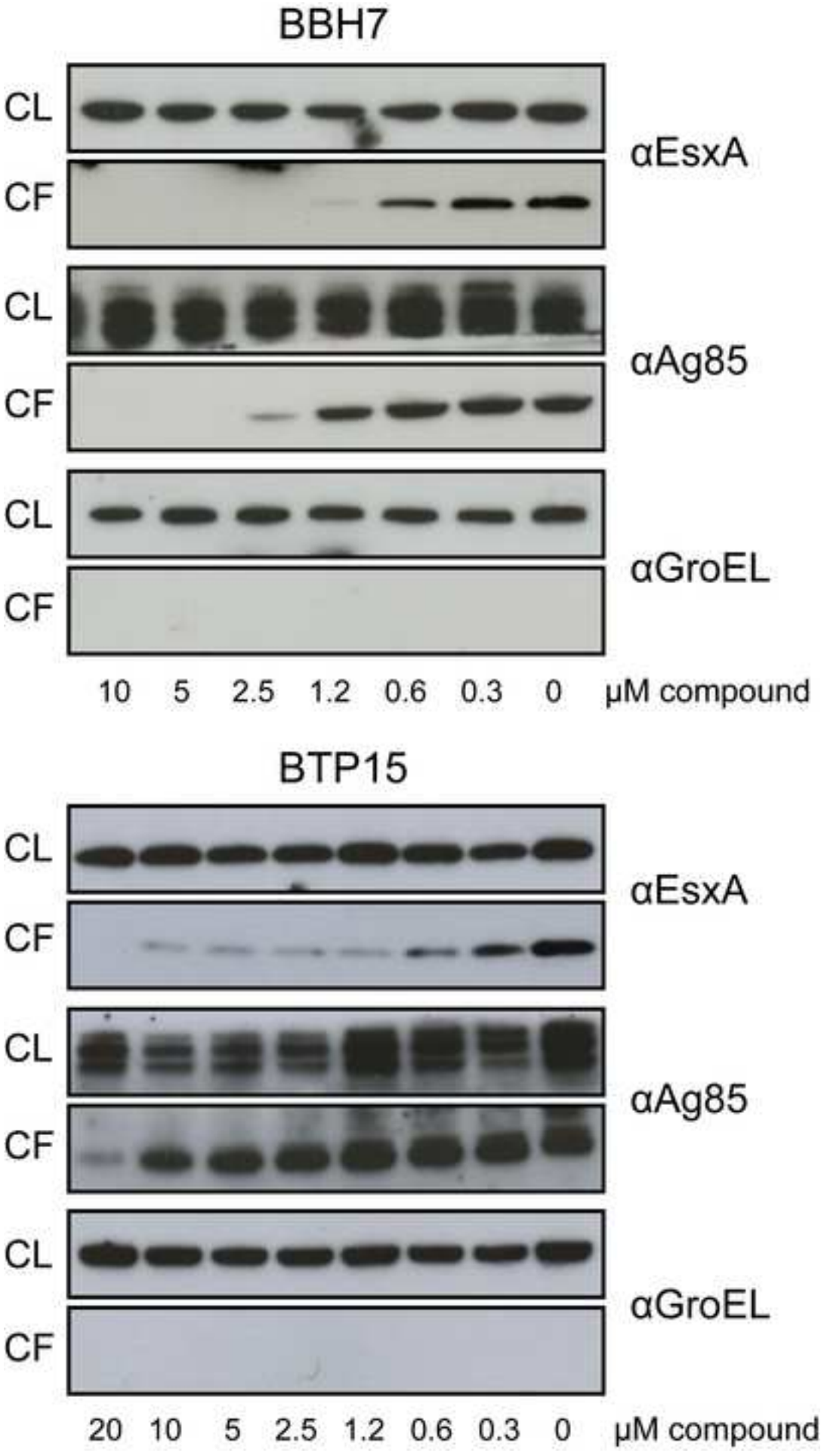

Figure 4
Click here to download high resolution image

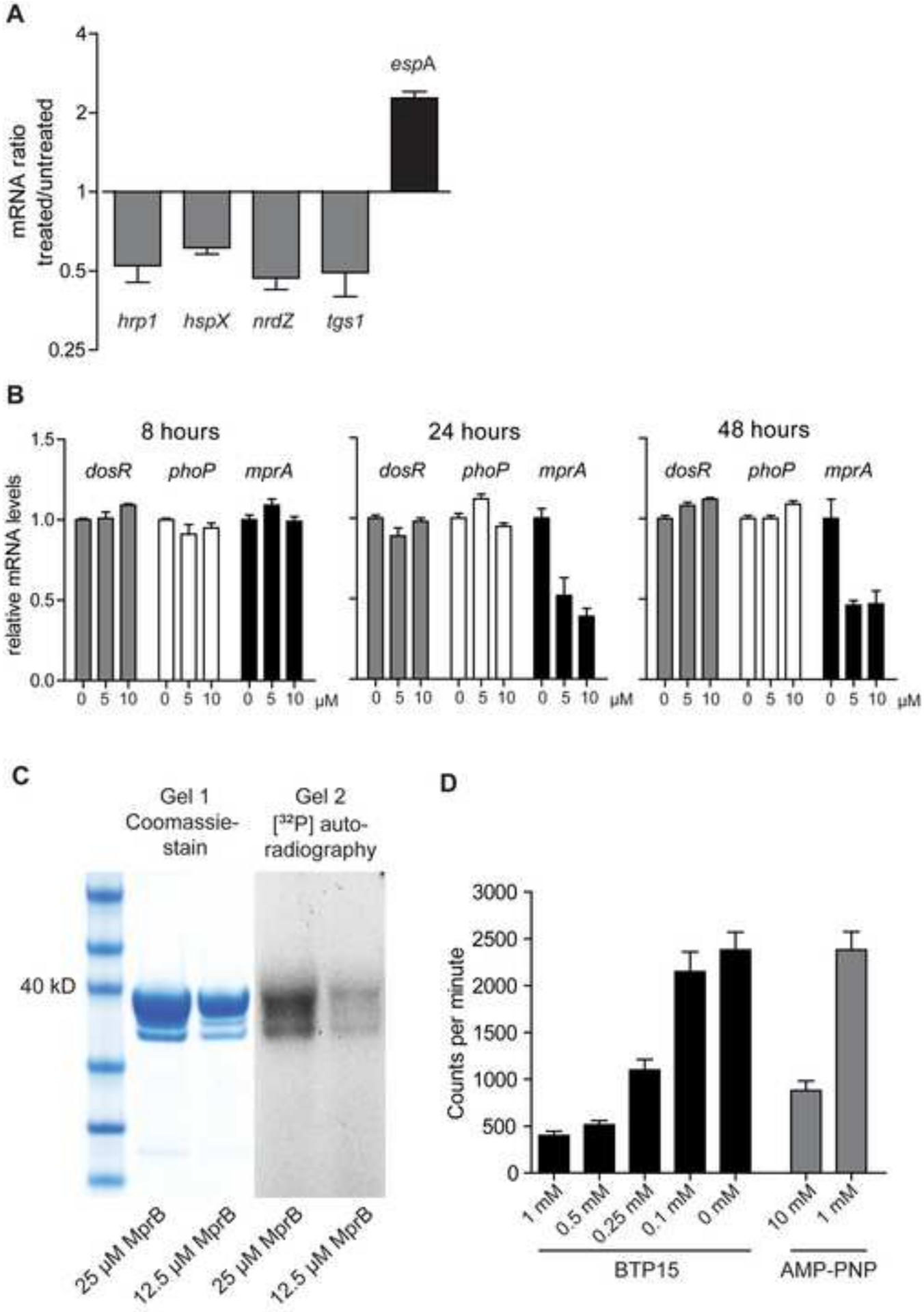

Figure 5
Click here to download high resolution image

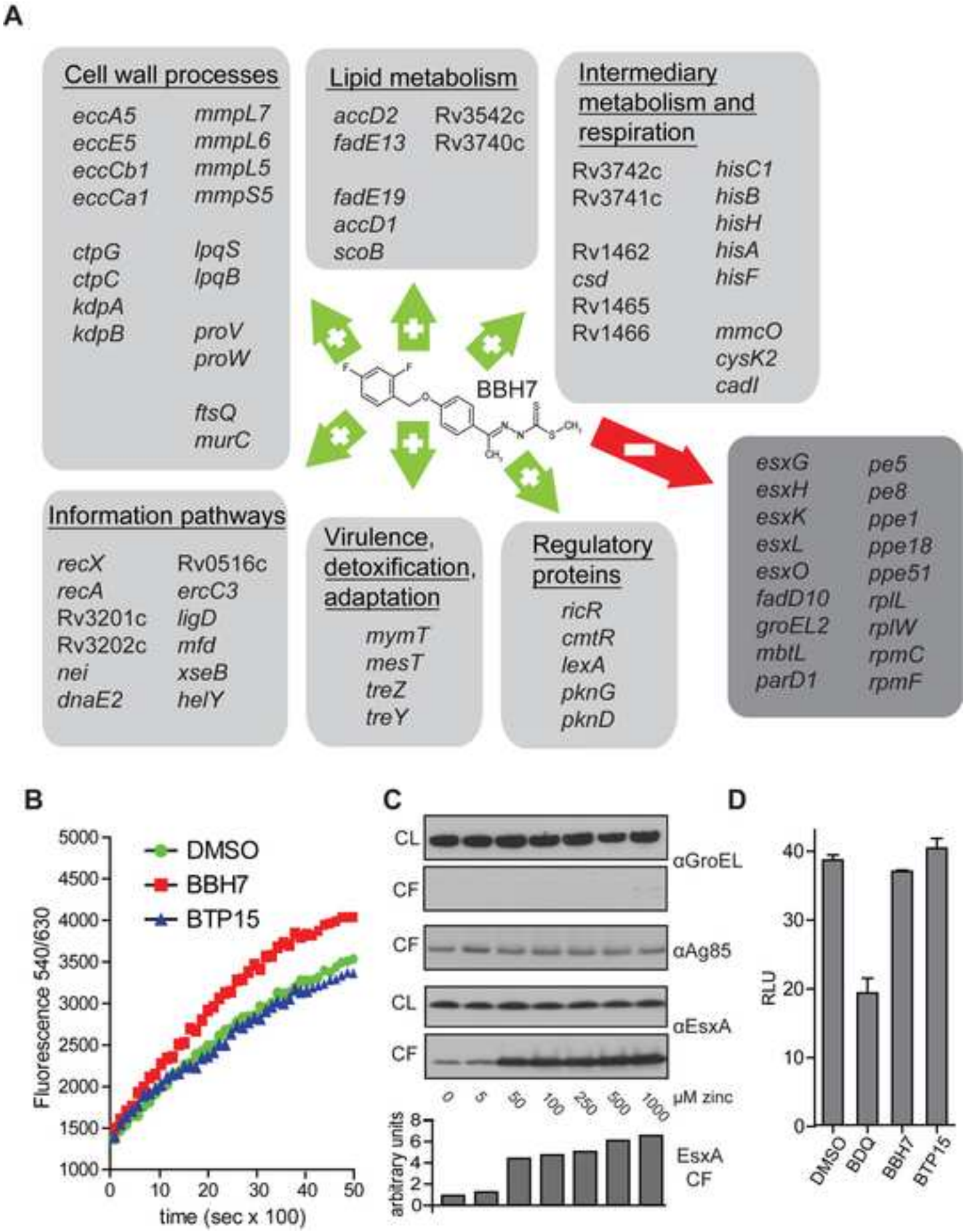

Figure 6
Click here to download high resolution image

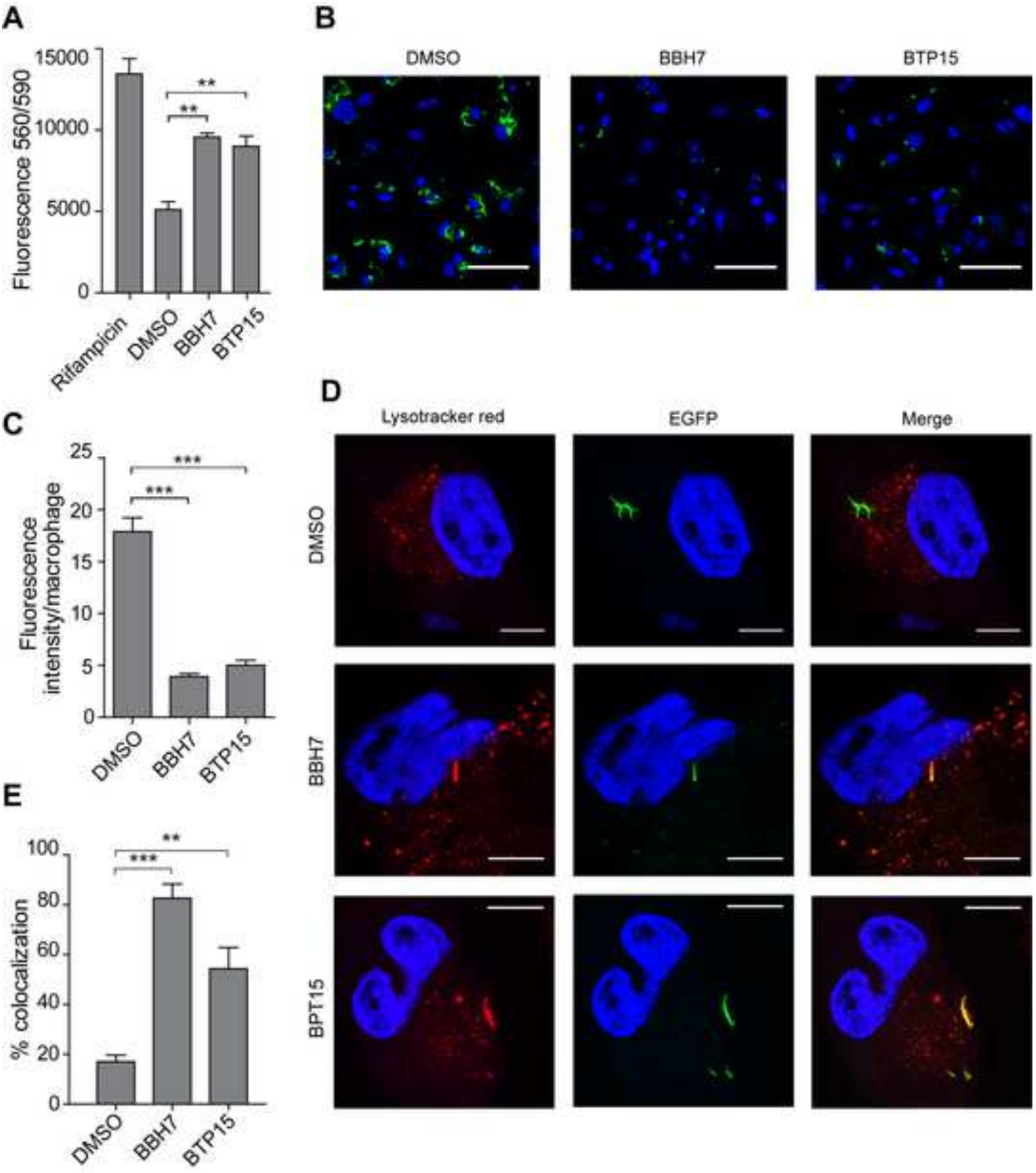

Figure 7
Click here to download high resolution image

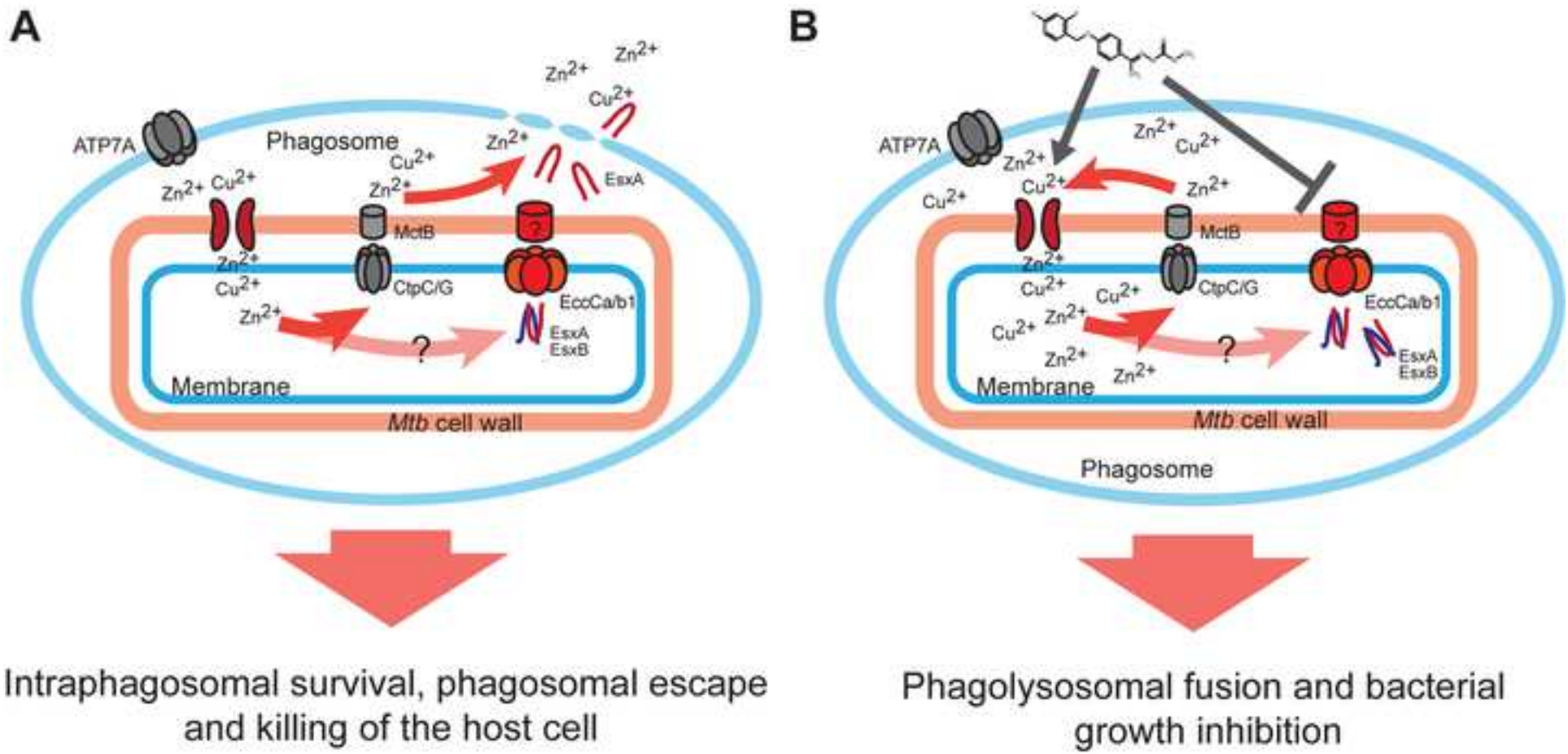

Intraphagosomal survival, phagosomal escape and killing of the host cell

Phagolysosomal fusion and bacterial growth inhibition

Supplemental information

Innovative anti-cytolytic screen identifies potent inhibitors of mycobacterial virulence protein secretion

Jan Rybniker, Jeffrey M. Chen, Claudia Sala, Ruben Hartkoorn, Anthony Vocat, Andrej Benjak, Stefanie Boy-Röttger, Ming Zhang, Rita E. Szekely, Zoltán Greff, László Örfi, István Szabadkai, János Pató, György Kéri, Stewart T. Cole

Supplemental inventory

Supplemental data:

Supplemental figures

Figure S1 (related to Figure 1). Activity of kinase inhibitors in the FSA; the Z'-factor of the FSA is > 0.5.

A. A selection of kinase inhibitors that are known to reduce the intracellular mycobacterial load in macrophages were screened in the FSA using an MOI of 10 and three days of incubation or an MOI of 2 and 5 days of incubation. There is only a slight protective effect of imatinib, H-89 and AX20017 after infection with an MOI of 2 (± SD). None of the compounds reduced mycobacterial growth in broth as determined in the REMA..

B. Z'-factor of the FSA was determined using 384 well plates and the controls DMSO (black data points) and rifampicin (red data points). Statistical calculations were done as described (Zhang et al., 1999). The Z'-factor of the displayed experiment is 0.626 indicating a high quality assay.

A

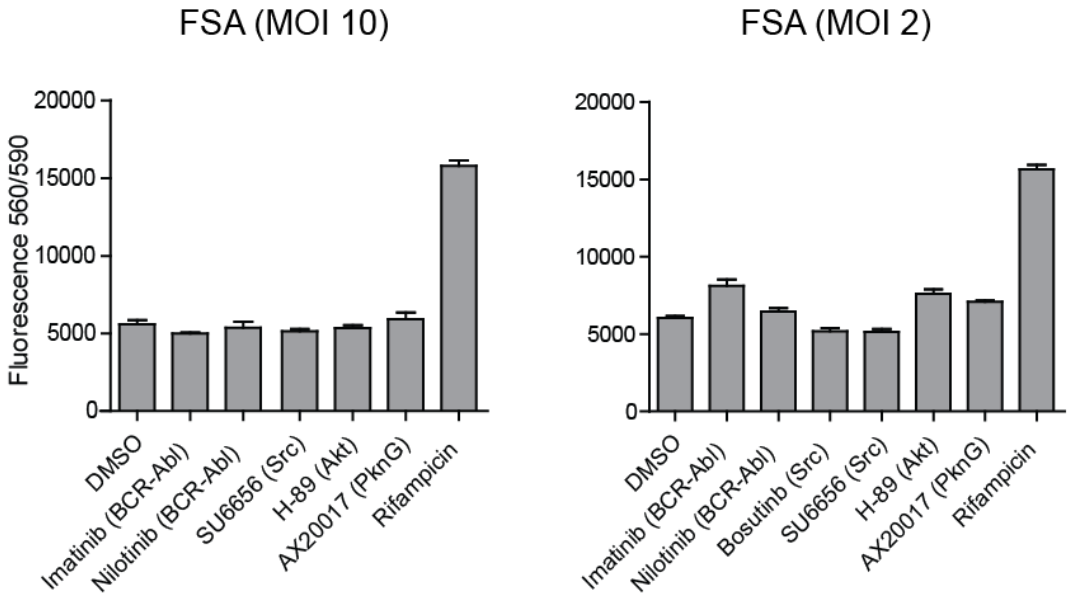
FSA (MOI 10)
Fluorescence 560/590
20000
15000
10000
5000
0
DMSO
Imatinib (BCR-Abl)
Nilotinib (BCR-Abl)
SU6656 (Src)
H-89 (Akt)
AX20017 (PknG)
Rifampicin

FSA (MOI 2)
20000
15000
10000
5000
0
DMSO
Imatinib (BCR-Abl)
Nilotinib (BCR-Abl)
Bosutinib (Src)
SU6656 (Src)
H-89 (Akt)
AX20017 (PknG)
Rifampicin

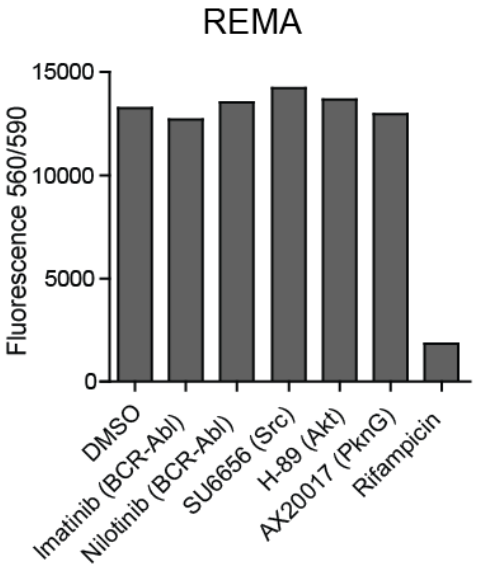
REMA
Fluorescence 560/590
15000
10000
5000
0
DMSO
Imatinib (BCR-Abl)
Nilotinib (BCR-Abl)
SU6656 (Src)
H-89 (Akt)
AX20017 (PknG)
Rifampicin

B

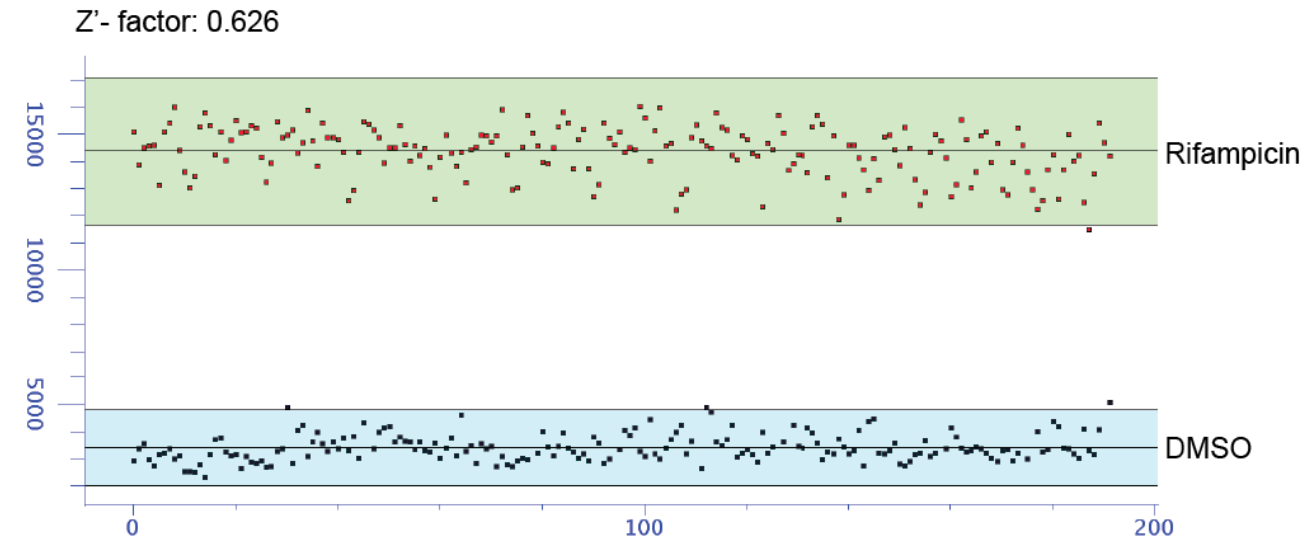
Z'- factor: 0.626
15000
10000
5000
Rifampicin
DMSO
0
100
200

Figure S2 (related to Figure 2). Molecular structures of BBH7 and BTP15.

A. Molecular structures of BBH7 and BTP15, both compounds are not growth inhibitory in broth. **B.** Growth curves of *Mtb*-Erdman treated with 25 µM of BTP15 or BBH7. The compounds are not growth inhibitory at concentrations that are 10x (BBH7) or 20x (BTP15) higher than the IC_{50} determined in the FSA. Rifampicin was used as a control at 5 µg/ml. Representative example of three individual experiments. **C.** MIC_{99} of BBH7 and BTP15 against a panel of mycobacterial and non-mycobacterial pathogens. Rifampicin (RIF) was used as a control.

A

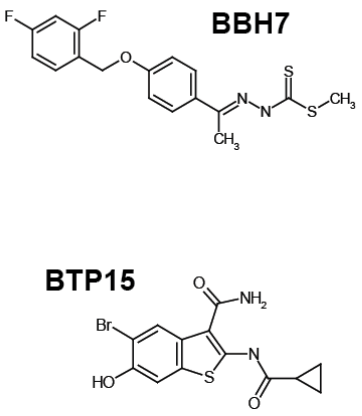

B

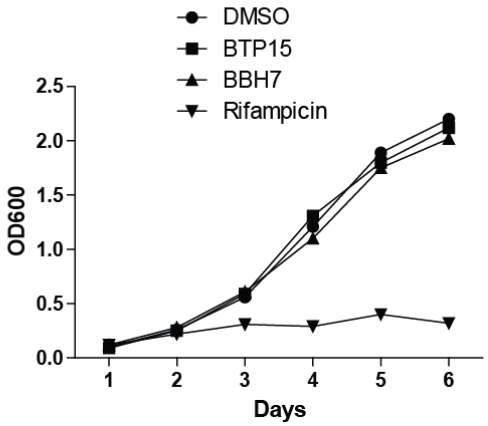

C

	MIC (µM)		
Strain	**BBH7**	**BTP15**	**RIF**
Mycobacterium bovis BCG	>100	>100	<0.2
Mycobacterium marinum strain M	>100	>100	<0.2
Mycobacterium smegmatis mc²155	>100	>100	1,6
Mycobacterium tuberculosis H37Rv	>100	>100	0,001
Bacillus subtilis	>100	>100	<0.2
Candida albicans	>100	>100	6,3
Corynebacterium diphtheriae	>100	>100	<0.2
Corynebacterium glutamicum	>100	>100	<0.2
Enterococcus faecalis	>100	>100	0,2
Listeria monocytogenes	>100	>100	0,4
Micrococcus Luteus	>100	>100	<0.2
Pseudomonas aeruginosa	>100	>100	6,3
Pseudomonas putida	>100	>100	3,1
Salmonella typhimurium	>100	>100	0,8
Staphylococcus aureus	>100	>100	3,1

Figure S3 (related to Figure 4). qRT-PCR of *mprB* after BTP15 treatment and anti-EspB Western blot of BTP15 treated samples

A. Transcription levels of *mprB* after 48 hours of treatment with 0, 5 and 10 µM of BTP15 determined by qRT-PCR. Data are derived from two biological replicates (± SD).

B. BTP15 inhibits EspB secretion as determined by Western blot. The faint upper band in the culture filtrate (CF) sample corresponds to uncleaved EspB.

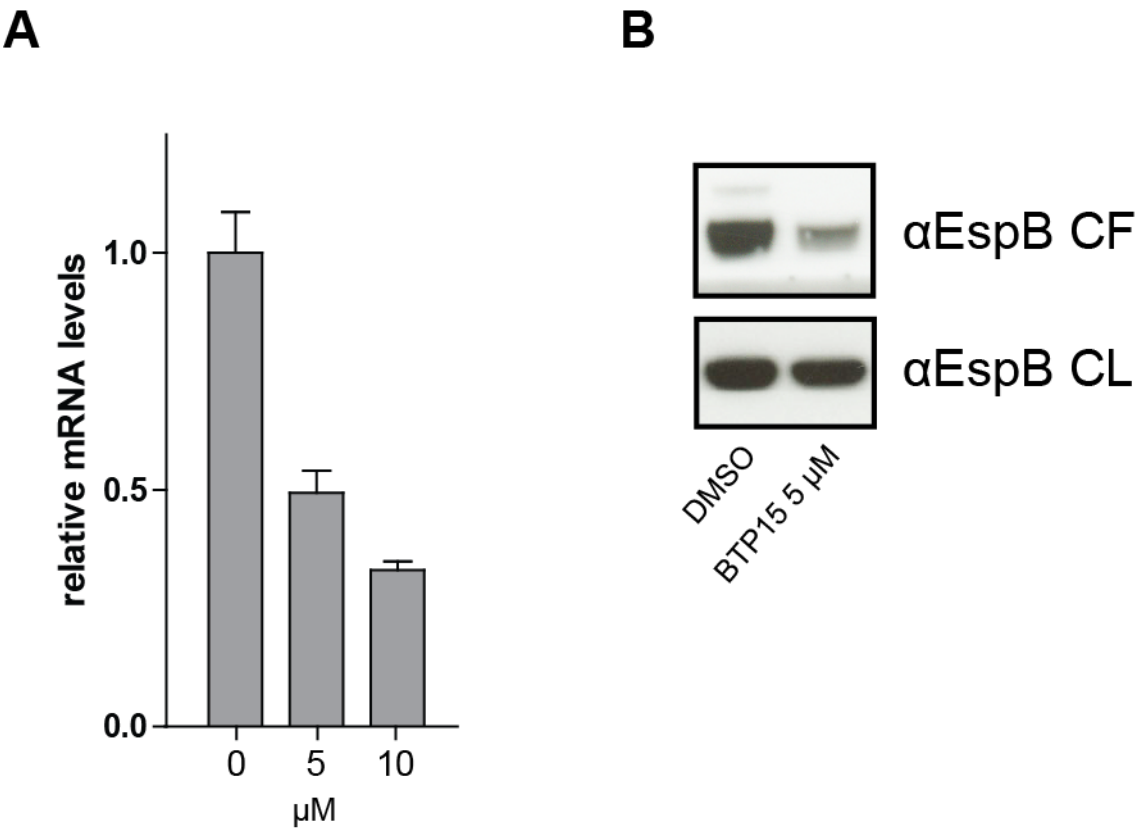

Figure S4 (related to Figure 5). Gene categories of BBH7-deregulated genes; confirmation by qRT-PCR and western blot targeting EsxA after treatment with cell wall inhibitors

A. Distribution of 144 BBH7 differentially regulated genes in different gene categories as determined by RNA-seq.

B. Transcription levels of differentially regulated genes upon BBH7 treatment determined by qRT-PCR. Data are derived from three biological replicates (± SD).

C. Western blot targeting EsxA in the culture filtrate of *Mtb*-treated with different cell wall biosynthesis inhibitors. EsxA and GroEL (lysis control) were detected in the culture filtrate of *Mtb*-Erdman treated with different cell wall biosynthesis inhibitors as well as BBH7 and BTP15, which are inhibitors of EsxA secretion (see Figure 3 of the main text). None of these well-described drugs have an impact on EsxA secretion. INH: Isoniazid, TAC: thioacetazone, ETH: ethionamide, EMB: ethambutol.

A

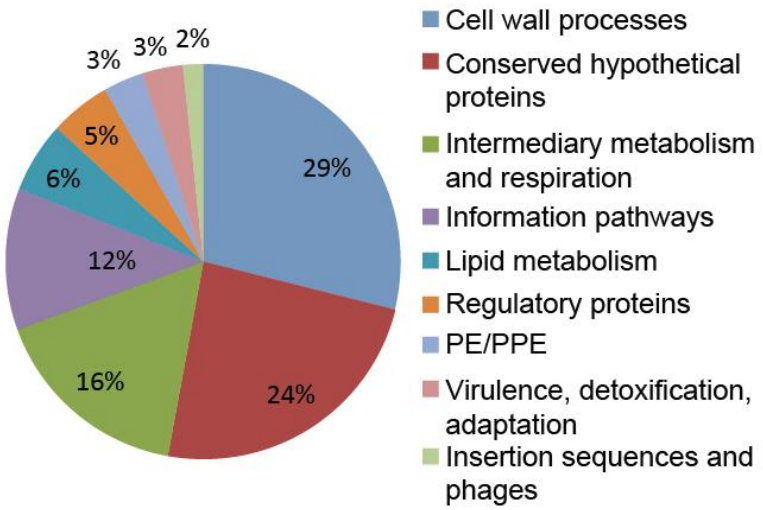
29%
24%
16%
12%
6%
5%
3%
3%
2%
Cell wall processes
Conserved hypothetical proteins
Intermediary metabolism and respiration
Information pathways
Lipid metabolism
Regulatory proteins
PE/PPE
Virulence, detoxification, adaptation
Insertion sequences and phages

B

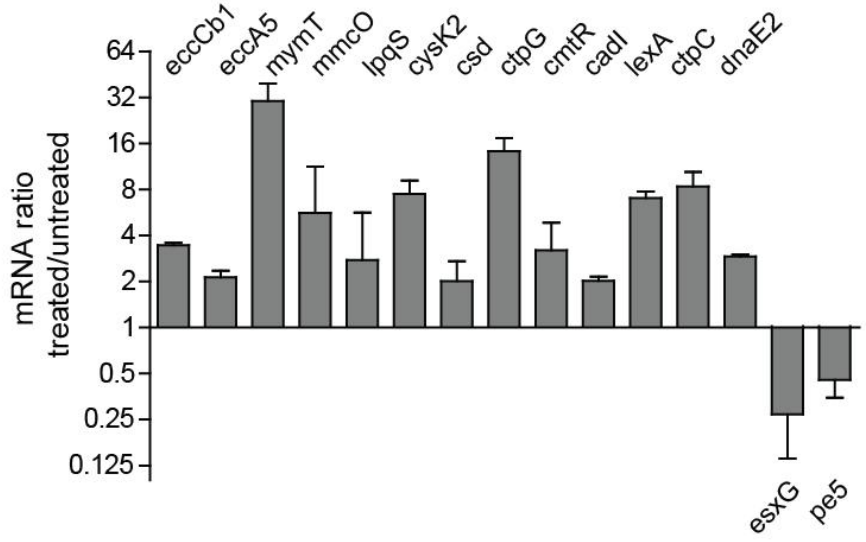
mRNA ratio treated/untreated
64
32
16
8
4
2
1
0.5
0.25
0.125
eccCb1
eccA5
mymT
mmcO
lpqS
cysK2
csd
ctpG
cmtR
cadI
lexA
ctpC
dnaE2
esxG
pe5

C

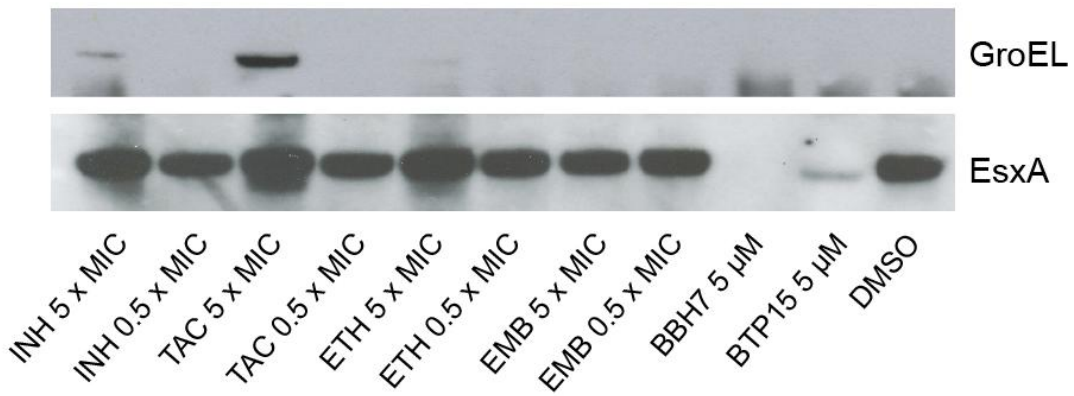
GroEL
EsxA
INH 5 x MIC
INH 0.5 x MIC
TAC 5 x MIC
TAC 0.5 x MIC
ETH 5 x MIC
ETH 0.5 x MIC
EMB 5 x MIC
EMB 0.5 x MIC
BBH7 5 µM
BTP15 5 µM
DMSO

Figure S5 (related to Figure 5). Effect of BBH7 on anti-TB-drugs

The MIC of five anti-TB-drugs was tested in the presence of 0, 10 and 25 µM of BBH7. BBH7 had no impact on the activity of these drugs.

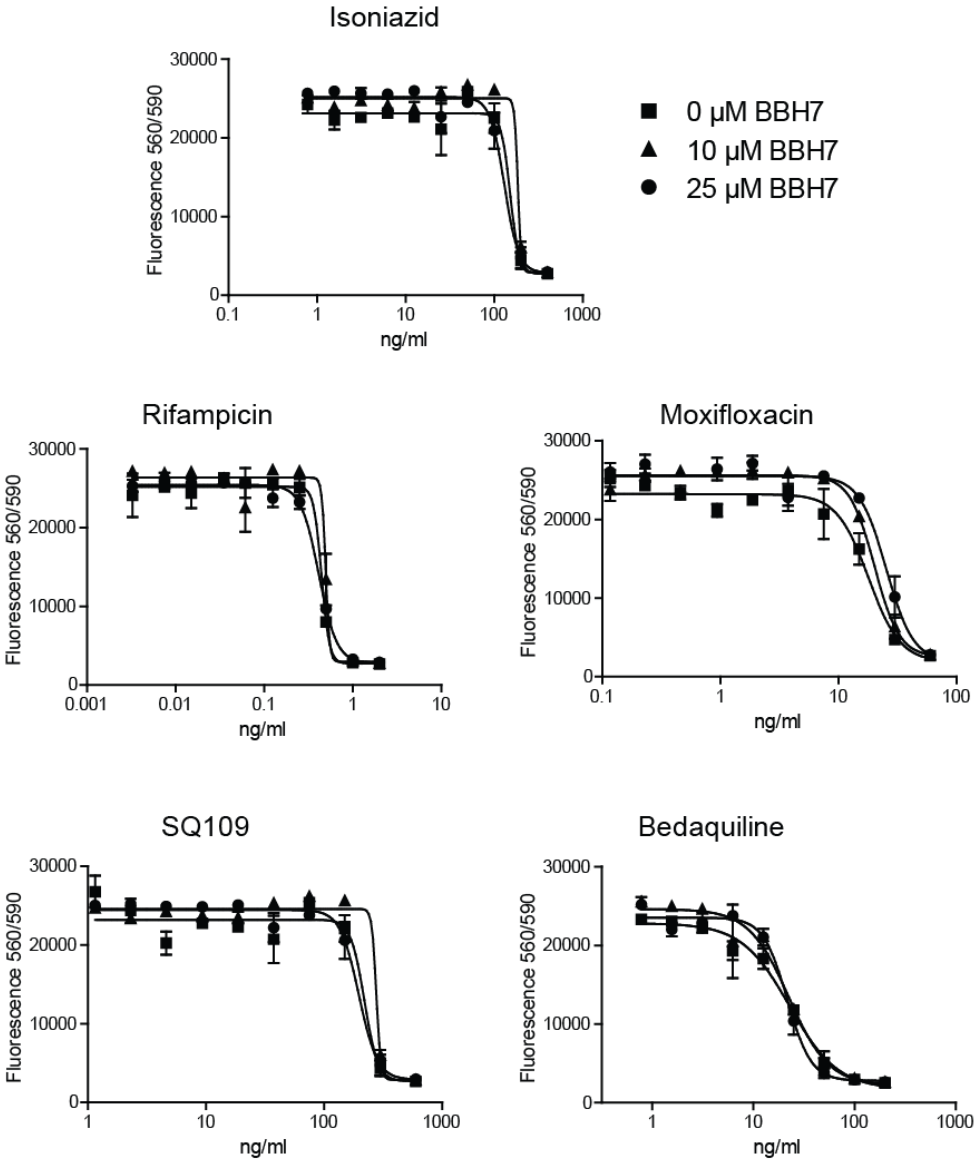

Table S1 (related to Figure 4). Differentially regulated genes after BTP15 treatment as determined by RNA-seq. Compound concentration was 5 µM (genes with > 1.5 fold differential regulation and an adjusted p-value of ≤ 0.01). Yellow label identifies genes which were shown to be differentially regulated in the Δ*mprAB* mutant strain under different conditions (He et al., 2006; Pang et al., 2007).

BTP15 downregulated genes

Id	Fold change	p-adjusted	transcript ID	function
Rv0569	0,387376749	2,72E-12	Rv0569	CONSERVED HYPOTHETICAL PROTEIN
Rv0570	0,465354705	2,92E-08	*nrdZ*	PROBABLE RIBONUCLEOSIDE-DIPHOSPHATE REDUCTASE (LARGE SUBUNIT)
Rv1733c	0,516776907	1,18E-05	Rv1733c	PROBABLE CONSERVED TRANSMEMBRANE PROTEIN
Rv1737c	0,564205063	0,0005607	*narK2*	POSSIBLE NITRATE/NITRITE TRANSPORTER NARK2
Rv1996	0,521345614	1,92E-05	Rv1996	CONSERVED HYPOTHETICAL PROTEIN
Rv2005c	0,59057313	0,0007544	Rv2005c	CONSERVED HYPOTHETICAL PROTEIN
Rv2030c	0,569889336	0,0005443	Rv2030c	CONSERVED HYPOTHETICAL PROTEIN
Rv2031c	0,557615907	8,87E-05	*hspX*	HEAT SHOCK PROTEIN HSPX (ALPHA-CRYSTALLIN HOMOLOG) (14 kDa ANTIGEN)
Rv2623	0,561569502	7,25E-05	TB31.7	CONSERVED HYPOTHETICAL PROTEIN TB31.7
Rv2624c	0,632962924	0,0103856	Rv2624c	CONSERVED HYPOTHETICAL PROTEIN
Rv2625c	0,55430127	7,98E-05	Rv2625c	PROBABLE CONSERVED TRANSMEMBRANE ALANINE AND LEUCINE RICH PROTEIN
Rv2626c	0,494421139	0,0138086	*hrp1*	HYPOXIC RESPONSE PROTEIN 1 HRP1
Rv2627c	0,540789469	3,17E-05	Rv2627c	CONSERVED HYPOTHETICAL PROTEIN
Rv2628	0,368669909	0,0043255	Rv2628	HYPOTHETICAL PROTEIN
Rv3127	0,605961489	0,0027788	Rv3127	CONSERVED HYPOTHETICAL PROTEIN
Rv3130c	0,562034139	8,87E-05	*tgs1*	TRIACYLGLYCEROL SYNTHASE (DIACYLGLYCEROL ACYLTRANSFERASE)
Rv3131	0,551127748	4,30E-05	Rv3131	CONSERVED HYPOTHETICAL PROTEIN
Rv3188	0,580839771	0,0075899	Rv3188	CONSERVED HYPOTHETICAL PROTEIN

BTP15 upregulated genes

Id	Fold change	p-adjusted	transcript ID	function
Rv0077c	2,63508874	1,04E-06	Rv0077c	PROBABLE OXIDOREDUCTASE
Rv0260c	2,013190924	0,005973739	Rv0260c	POSIBLE TRANSCRIPTIONAL REGULATORY PROTEIN
Rv0560c	8,271819287	5,30E-16	Rv0560c	POSSIBLE BENZOQUINONE METHYLTRANSFERASE (METHYLASE)
Rv0711	2,032490101	7,38E-06	*atsA*	POSSIBLE ARYLSULFATASE ATSA (ARYL-SULFATE SULPHOHYDROLASE)
Rv1039c	2,674652601	7,38E-06	*PPE15*	PPE FAMILY PROTEIN
Rv1040c	2,106243566	2,34E-05	*PE8*	PE FAMILY PROTEIN
Rv1168c	2,462735966	1,44E-10	*PPE17*	PPE FAMILY PROTEIN
Rv1169c	2,149757072	0,011485251	*lipX*	PE FAMILY PROTEIN. POSSIBLE LIPASE.
Rv1221	2,0231764319	0,001087853	*sigE*	ALTERNATIVE RNA POLYMERASE SIGMA FACTOR SIGE
Rv1471	1,650888992	0,011972813	*trxB1*	PROBABLE THIOREDOXIN TRXB1
Rv1557	8,381628918	2,31E-48	*mmpL6*	PROBABLE CONSERVED TRANSMEMBRANE TRANSPORT PROTEIN MMPL6
Rv2025c	1,67335257	0,002223857	Rv2025c	POSSIBLE CONSERVED MEMBRANE PROTEIN
Rv2466c	2,030361839	0,00060111	Rv2466c	CONSERVED HYPOTHETICAL PROTEIN
Rv3340	1,867363035	3,37E-05	*metC*	PROBABLE O-ACETYLHOMOSERINE SULFHYDRYLASE METC
Rv3463	2,276705761	2,24E-08	Rv3463	CONSERVED HYPOTHETICAL PROTEIN
Rv3833	2,015199778	0,000187711	Rv3833	TRANSCRIPTIONAL REGULATORY PROTEIN (PROBABLY ARAC-FAMILY)
Rv3913	1,707746392	0,001499179	*trxB2*	PROBABLE THIOREDOXIN REDUCTASE TRXB2 (TRXR) (TR)

Table S2 (related to Figure 5). Secretome analysis of BBH7-treated bacteria

A selection of secreted proteins which were quantified at lower amounts in the culture filtrate of BBH7-treated bacteria (compound concentration 5 µM). Data are derived from two biological replicates; proteins were identified by LC-MS/MS as described in the supplementary methods.

Id	Name	Ratio treated/ untreated	Product	Function	Secretion system
Rv0129c	Ag85C	-4.75	mycolyltransferase	Involved in cell wall synthesis	Tat substrate
Rv0164	TB18.5	-3.13	unknown	Predicted outer membrane protein, essential gene in vitro, CD8+ and CD4+ T-cell epitope in mice	unknown
Rv1793	EsxN	-4.95	unknown	EsxA like proteins	ESX-5
Rv2145c	Wag31	-3.48	unknown	Probably involved in cell division process. Essential gene in vitro	unknown
Rv1792	EsxM	-5,02	unknown	EsxA like protein	ESX-5
Rv2430c	PPE41	-3.8	unknown	PPE family protein, ESX-5 secretion deficiency leads to attenuation in vivo and disruption of cell wall integrity	ESX-5
Rv2431c	PE25	-4.23	unknown	PE family protein, ESX-5 secretion deficiency leads to attenuation in vivo and disruption of cell wall integrity	ESX-5
Rv2525c	Rv2525c	-2.80	unknown	Possible role in biosynthesis of the cell wall, deletion results in enhanced susceptibility to beta-lactam antibiotics	Predicted Tat substrate
Rv3208A	TB9.4	-4.17	unknown	unknown	unknown
Rv3451	Cut3	-4.3	Probable cutinase precursor	Hydrolysis of cutin	ESX-5
Rv3682	PonA2	-3.19	penicillin-binding protein, membrane-associated, transglycosylase and transpeptidase activities	Required for survival in primary murine macrophages	unknown
Rv3881c	EspB	-3.63	unknown	Essential for secretion of EsxA	ESX-1

Table S3 (related to Figure 5). Differentially regulated genes after BBH7 treatment as determined by RNA-seq. Compound concentration was 5 µM (genes with > 2 fold differential regulation and an adjusted p-value of ≤ 0.01).

A. Up-regulated genes

id	transcript id	pval	padj	start	stop	fold change	function	gene category
Rv0047c	Rv0047c	4,57E-07	2,77E-05	51185	51727	2,511884581	CONSERVED HYPOTHETICAL PROTEIN	Conserved hypthetical s
Rv0077c	Rv0077c	1,26E-24	5,81E-22	85636	86466	6,345746181	PROBABLE OXIDOREDUCTASE	intermediary metabolism and respiration
Rv0186A	mymT	7,35E-61	2,03E-57	218390	218551	19,62868205	METALLOTHIONEIN, MYMT	virulence, detoxification, adaptation
Rv0190	Rv0190	1,68E-05	1,36E-03	221871	222161	2,668253476	CONSERVED HYPOTHETICAL PROTEIN	cell wall and cell processes
Rv0336	Rv0336	4,65E-22	1,69E-19	400192	401703	4,858488205	CONSERVED 13 E1/2 REPEAT FAMILY PROTEIN	insertion seqs and phages
Rv0354c	PPE7	0,000018834	0,004974424	426359	426694	2,476064139	PPE FAMILY PROTEIN	PE/PPE
Rv0355c	PPE8	1,47E-06	8,03E-05	424777	434679	2,083253888	PPE FAMILY PROTEIN	PE/PPE
Rv0410c	pknG	3,50E-09	3,31E-07	495052	497314	2,416941158	SERINE/THREONINE-PROTEIN KINASE PKNG (PROTEIN KINASE G) (STPK G)	regulatory proteins
Rv0511	hemD	1,12E-06	6,20E-05	602819	604516	2,103485118	PROBABLE UROPORPHYRIN-III C-METHYLTRANSFERASE HEMD (UROPORPHYRI	intermediary metabolism and respiration
Rv0512	hemB	2,79E-08	2,09E-06	604602	605591	2,571564274	PROBABLE DELTA-AMINOLEVULINIC ACID DEHYDRATASE HEMB (PORPHOBILIN	intermediary metabolism and respiration
Rv0516c	Rv0516c	1,12E-18	2,77E-16	603052	603535	4,432653686	POSSIBLE ANTI-ANTI-SIGMA FACTOR	information pathways
Rv0526	Rv0526	3,38E-05	0,001185 3	616846	617493	2,087454478	POSSIBLE THIOREDOXIN PROTEIN (THIOL-DISULFIDE INTERCHANGE PROTEIN)	intermediary metabolism and respiration
Rv0676c	mmpL5	1,91E-33	1,65E-30	775586	778477	6,630272362	PROBABLE CONSERVED TRANSMEMBRANE TRANSPORT PROTEIN MMPL5	cell wall and cell processes
Rv0677c	mmpS5	9,01E-23	3,46E-20	778480	778905	4,682226367	POSSIBLE CONSERVED MEMBRANE PROTEIN MMPS5	cell wall and cell processes
Rv0678	Rv0678	2,76E-23	1,16E-20	778990	779487	4,825234512	CONSERVED HYPOTHETICAL PROTEIN	Conserved hypthetical s
Rv0846c	mmaO	3,48E-15	6,68E-13	942680	944194	3,72396729	PROBABLE OXIDASE	intermediary metabolism and respiration
Rv0847	lpqS	3,64E-28	2,23E-25	944343	944735	6,125739687	PROBABLE LIPOPROTEIN LPQS	cell wall and cell processes
Rv0848	cysK2	6,24E-19	1,66E-16	944938	945956	5,113026242	POSSIBLE CYSTEINE SYNTHASE A CYSK2 (O-ACETYLSERINE SULFHYDRYLASE) (O	intermediary metabolism and respiration
Rv0849	Rv0849	1,16E-10	1,45E-08	945956	947312	4,670901479	PROBABLE CONSERVED INTEGRAL MEMBRANE TRANSPORT PROTEIN	cell wall and cell processes
Rv0961c	ercc3	2,18E-11	3,01E-09	958523	960151	3,091206846	PROBABLE DNA HELICASE ERCC3	information pathways
Rv0875c	Rv0875c	1,93E-05	0,000721 2	973806	974291	2,018083961	POSSIBLE CONSERVED EXPORTED PROTEIN	cell wall and cell processes
Rv0906	Rv0906	7,84E-10	8,21E-08	1003944	1010062	2,695619529	CONSERVED HYPOTHETICAL PROTEIN	cell wall and cell processes
Rv0913c	Rv0913c	3,54E-07	2,19E-05	1017217	1018725	2,165291864	POSSIBLE DIOXYGENASE	intermediary metabolism and respiration
Rv0931c	pknD	7,43E-08	5,27E-06	1057925	1038914	2,200424108	TRANSMEMBRANE SERINE/THREONINE-PROTEIN KINASE D PKND (PROTEIN KI	regulatory proteins
Rv0938	lgt0	9,39E-08	6,56E-06	1046136	1048412	2,258734401	ATP DEPENDENT DNA LIGASE (ATP DEPENDENT POLYDEOXYRIBONUCLEOTIDE	information pathways
Rv0974c	accD2	0,000143 5	0,003994 7	1085756	1087345	2,377977856	PROBABLE ACETYL-/PROPIONYL-CoA CARBOXYLASE (BETA SUBUNIT) ACCD2	lipid metabolism
Rv0975c	fadE13	0,000171 5	0,004597 1	1087348	1088493	2,541155833	PROBABLE ACYL-CoA DEHYDROGENASE FADE13	lipid metabolism
Rv1000c	Rv1000c	6,03E-14	9,82E-12	1116531	1117148	4,421266263	CONSERVED HYPOTHETICAL PROTEIN. THOUGHT TO BE REGULATED BY Rv2720	Conserved hypthetical s
Rv1020	mfd	1,16E-11	1,63E-09	1138967	1142571	2,892043196	PROBABLE TRANSCRIPTION-REPAIR COUPLING FACTOR MFD (TRCF)	information pathways
Rv1021	Rv1021	2,76E-08	2,03E-06	1142671	1143648	2,532989058	CONSERVED HYPOTHETICAL PROTEIN	Conserved hypthetical s
Rv1029	kdpA	9,72E-12	1,39E-09	1152012	1153724	3,782451076	Probable Potassium-transporting ATPase A chain KDPA (ATP phospholy hydrolase	cell wall and cell processes
Rv1030	kdpB	1,40E-07	9,44E-06	1153727	1155853	2,805631721	Probable Potassium-transporting P-type ATPase B chain KDPB (Potassium-tran	cell wall and cell processes
Rv1107c	xseB	7,34E-05	0,000312 3	1233966	1234213	2,204721057	PROBABLE EXODEOXYRIBONUCLEASE VII (SMALL SUBUNIT) XSEA (EXONUCLEA	information pathways
Rv1173	fbiC	1,46E-05	7,97E-04	1302931	1305501	2,070768558	PROBABLE F420 BIOSYNTHESIS PROTEIN FBIC	intermediary metabolism and respiration
Rv1217c	Rv1217c	1,18E-05	6,49E-04	1360155	1361798	2,468085881	PROBABLE TETRONASIN-TRANSPORT INTEGRAL MEMBRANE PROTEIN ABC TR	cell wall and cell processes
Rv1218c	Rv1218c	0,000022 34	0,001748 96	1361801	1362725	2,01548372	PROBABLE TETRONASIN-TRANSPORT ATP-BINDING PROTEIN ABC TRANSPORT	cell wall and cell processes
Rv1219c	Rv1219c	0,000018 17	0,001482 53	1362733	1363361	2,171766507	PROBABLE TRANSCRIPTIONAL REGULATORY PROTEIN	regulatory proteins
Rv1378c	Rv1378c	2,65E-10	3,03E-08	1551228	1552654	6,933503995	CONSERVED HYPOTHETICAL PROTEIN	Conserved hypthetical s
Rv1462	Rv1462	6,37E-09	5,64E-07	1649529	1650716	2,388 2 05555	CONSERVED HYPOTHETICAL PROTEIN	intermediary metabolism and respiration
Rv1463	Rv1463	1,15E-09	1,17E-07	1650719	1651516	2,557 158036	POSSIBLE CONSERVED ATP-BINDING PROTEIN ABC TRANSPORTER	cell wall and cell processes
Rv1464	csd	5,21E-10	5,63E-08	1651518	1652768	2,588 164866	PROBABLE CYSTEINE DESULFURASE CSD	intermediary metabolism and respiration
Rv1465	Rv1465	2,17E-06	0,000111 22	1652771	1653231	2,274494611	POSSIBLE NITROGEN FIXATION RELATED PROTEIN	intermediary metabolism and respiration
Rv1466	Rv1466	3,32E-05	0,001170 18	1653256	1653578	2,000167453	CONSERVED HYPOTHETICAL PROTEIN	intermediary metabolism and respiration
Rv1481	Rv1481	3,41E-05	0,001195 8	1671377	1672584	2,020292633	PROBABLE MEMBRANE PROTEIN	cell wall and cell processes
Rv1557	mmpL6	2,64E-51	5,21E-48	1761744	1762937	13,93539757	PROBABLE CONSERVED TRANSMEMBRANE TRANSPORT PROTEIN MMPL6	cell wall and cell processes
Rv1562c	treZ	5,44E-05	0,001779	1765400	1767135	2,330028794	Maltooligosyltrehalose trehalohydrolase TreZ	virulence, detoxification, adaptation
Rv1563c	treY	0,000837 22	0,008861 2	1767142	1769432	2,035122372	Maltooligosyltrehalose synthase TreY	virulence, detoxification, adaptation
Rv1565c	Rv1565c	1,30E-06	7,13E-05	1771640	1773829	2,100221473	CONSERVED HYPOTHETICAL MEMBRANE PROTEIN	cell wall and cell processes
Rv1600	hisC1	2,36E-07	1,53E-05	1802899	1802035	2,195548653	Probable histidinol-phosphate aminotransferase hisC1	intermediary metabolism and respiration
Rv1601	hisB	2,93E-10	3,35E-08	1802038	1802564	2,813904191	Probable imidazoleglycerol-phosphate dehydratase hisB	intermediary metabolism and respiration
Rv1602	hisH	5,59E-07	3,32E-05	1802567	1803284	2,297187241	Probable amidotransferase hisH	intermediary metabolism and respiration
Rv1603	hisA	4,18E-07	2,57E-05	1803294	1804031	2,347058518	PROBABLE PHOSPHORIBOSYLFORMIMINO-5-AMINOIMIDAZOLE CARBOXAMIDE	intermediary metabolism and respiration
Rv1604	impA	3,80E-09	3,58E-07	1804039	1804851	2,679248751	PROBABLE INOSITOL-MONOPHOSPHATASE IMPA (IMP)	cell wall and cell processes
Rv1605	hisF	4,28E-09	3,97E-07	1804853	1805653	2,743882893	Probable cyclase hisF	intermediary metabolism and respiration
Rv1686c	Rv1686c	2,02E-05	0,001105 6	1911401	1912081	2,222765 21	PROBABLE CONSERVED INTEGRAL MEMBRANE PROTEIN ABC TRANSPORTER	cell wall and cell processes
Rv1702c	Rv1702c	2,95E-23	1,20E-20	1927211	1928575	5,870518875	CONSERVED HYPOTHETICAL PROTEIN	insertion seqs and phages
Rv1773c	Rv1773c	3,70E-06	0,000178 2	2007020	2007766	2,197117029	PROBABLE TRANSCRIPTIONAL REGULATORY PROTEIN	regulatory proteins
Rv1787	PPE25	9,28E-05	0,002810 1	2025301	2026398	2,32353404	PPE FAMILY PROTEIN	PE/PPE
Rv1790	PPE27	1,61E-05	0,000616 28	2028425	2029477	3,139265201	PPE FAMILY PROTEIN	PE/PPE
Rv1797	eccE5	5,43E-06	0,000241 3	2035486	2036700	2,026851647	ESX CONSERVED COMPONENT ECCE5. PROBABLE MEMBRANE PROTEIN.	cell wall and cell processes
Rv1798	eccA5	1,90E-07	1,25E-05	2036703	2038532	2,257891815	ESX CONSERVED COMPONENT ECCA5	cell wall and cell processes
Rv1813c	Rv1813c	8,44E-22	2,92E-19	2055681	2056112	5,486316956	CONSERVED HYPOTHETICAL PROTEIN	Conserved hypthetical s
Rv1992c	ctpG	2,10E-46	3,22E-43	2234991	2237303	9,975382044	PROBABLE METAL CATION TRANSPORTER P-TYPE ATPASE G CTPG	cell wall and cell processes
Rv1993c	Rv1993c	5,21E-16	2,77E-13	2237306	2237575	5,500610878	CONSERVED HYPOTHETICAL PROTEIN	Conserved hypthetical s
Rv1994c	cmtR	1,30E-19	3,76E-17	2237628	2237984	4,459152486	METAL SENSOR TRANSCRIPTIONAL REGULATOR CMTR (ARSR-SMTB FAMILY)	regulatory proteins
Rv2024c	Rv2024c	9,70E-09	8,29E-07	2268726	2270240	2,542396025	CONSERVED HYPOTHETICAL PROTEIN	Conserved hypthetical s
Rv2025c	Rv2025c	5,55E-23	2,20E-20	2270750	2271748	4,520834842	POSSIBLE CONSERVED MEMBRANE PROTEIN	cell wall and cell processes
Rv2029c	helY	1,09E-14	1,95E-12	2349334	2352054	3,700276251	PROBABLE ATP-DEPENDENT DNA HELICASE HELY	information pathways
Rv2151c	ftsQ	3,93E-05	0,001345	2409697	2410638	2,35801176	POSSIBLE CELL DIVISION PROTEIN FTSQ	cell wall and cell processes
Rv2152c	murC	1,49E-07	9,94E-06	2410641	2412119	2,344249563	Probable UDP-N-acetylmuramate-alanine ligase MurC	cell wall and cell processes
Rv2240c	glpD1	0,000022 86	0,001748 96	2523241	2524785	2,244193138	PROBABLE GLYCEROL-3-PHOSPHATE DEHYDROGENASE GLPD1	intermediary metabolism and respiration
Rv2364c	era	1,27E-14	2,25E-12	2645774	2646673	4,047002053	PROBABLE GTP-BINDING PROTEIN ERA	intermediary metabolism and respiration
Rv2365c	Rv2365c	6,37E-08	4,57E-06	2646747	2647060	3,957522614	CONSERVED HYPOTHETICAL PROTEIN	Conserved hypthetical s
Rv2366c	Rv2366c	1,93E-08	1,52E-06	2647088	2648364	2,56594474	PROBABLE CONSERVED TRANSMEMBRANE PROTEIN	cell wall and cell processes
Rv2499c	Rv2499c	6,80E-05	0,003290 1	2813176	2813727	2,191289454	POSSIBLE OXIDASE REGULATORY-RELATED PROTEIN	intermediary metabolism and respiration
Rv2500c	fadE19	2,91E-07	1,84E-05	2813730	2814911	2,180313107	POSSIBLE ACYL-CoA DEHYDROGENASE FADE19 (MMGC)	lipid metabolism
Rv2502c	accD1	3,31E-07	2,05E-05	2816885	2818471	2,348009195	PROBABLE ACETYL-/PROPIONYL-CoA CARBOXYLASE (BETA SUBUNIT) ACCD1	lipid metabolism
Rv2503c	scoB	7,92E-07	4,57E-05	2818474	2819124	2,282035468	PROBABLE SUCCINYL-COA:3-KETOACID-COENZYME A TRANSFERASE (BETA SU	lipid metabolism
Rv2578c	Rv2578c	9,71E-31	7,07E-28	2902509	2903531	9,456571701	CONSERVED HYPOTHETICAL PROTEIN	Conserved hypthetical s
Rv2641	cadI	2,48E-09	2,29E-07	2965939	2966397	2,434465033	CADMIUM INDUCIBLE PROTEIN CADI	Conserved hypthetical s
Rv2719c	Rv2719c	5,79E-10	6,21E-08	3031040	3031537	3,215033848	POSSIBLE CONSERVED MEMBRANE PROTEIN	cell wall and cell processes
Rv2720	lexA	1,22E-17	2,81E-15	3031788	3032498	3,948140168	REPRESSOR LEXA	regulatory proteins
Rv2735c	Rv2735c	4,63E-09	4,24E-07	3047675	3048552	2,911323572	CONSERVED HYPOTHETICAL PROTEIN	Conserved hypthetical s
Rv2736c	recX	5,49E-05	0,001787 3	3048556	3049052	2,068335667	REGULATORY PROTEIN RECX	information pathways
Rv2737c	recA	1,95E-08	1,53E-06	3049086	3051424	2,364400641	RECA PROTEIN (RECOMBINASE A) (CONTAINS: ENDONUCLEASE PI-MTUI (MTU	information pathways
Rv2826c	Rv2826c	9,64E-05	0,003093 1	3133709	3134593	2,557 189294	HYPOTHETICAL PROTEIN	Conserved hypthetical s
Rv2942	mmpL7	8,67E-09	7,54E-07	3285077	3287832	2,372859046	CONSERVED TRANSMEMBRANE TRANSPORT PROTEIN MMPL7	cell wall and cell processes
Rv2963	Rv2963	7,44E-16	1,51E-13	3315256	3316456	9,716425183	PROBABLE INTEGRAL MEMBRANE PROTEIN	cell wall and cell processes
Rv2964	purU	3,92E-10	4,31E-08	3316529	3317461	2,870810059	PROBABLE FORMYLTETRAHYDROFOLATE DEFORMYLASE PURU (FORMYL-FH(4)	intermediary metabolism and respiration
Rv3074	Rv3074	1,41E-22	5,27E-20	3436779	3438050	8,074725837	CONSERVED HYPOTHETICAL PROTEIN	Conserved hypthetical s
Rv3176c	mesT	1,59E-09	1,59E-07	3544347	3545300	3,077018966	PROBABLE EPOXIDE HYDROLASE MEST (EPOXIDE HYDRATASE) (ARENE-OXIDE	virulence, detoxification, adaptation
Rv3201c	Rv3201c	2,50E-07	1,80E-05	3573731	3577033	2,796895258	PROBABLE ATP-DEPENDENT DNA HELICASE	information pathways
Rv3202c	Rv3202c	1,03E-07	7,13E-06	3577086	3580200	3,338118983	4 POSSIBLE ATP-DEPENDENT DNA HELICASE	information pathways
Rv3212	Rv3212	1,53E-06	8,27E-05	3589394	3590617	2,772919889	CONSERVED HYPOTHETICAL ALANINE/VALINE RICH PROTEIN	Conserved hypthetical s
Rv3244c	lprB	2,76E-08	2,03E-06	3625159	3626410	2,362080961	PROBABLE CONSERVED LIPOPROTEIN LPQB	cell wall and cell processes
Rv3270	ctpC	1,40E-18	3,41E-16	3650526	3652679	3,796256206	PROBABLE METAL CATION-TRANSPORTING P-TYPE ATPASE C CTPC	cell wall and cell processes
Rv3289c	Rv3289c	1,12E-05	9,41E-04	3670084	3670411	2,429642446	POSSIBLE TRANSMEMBRANE PROTEIN	cell wall and cell processes
Rv3290c	lat	1,77E-06	9,36E-05	3670445	3671794	2,025758507	PROBABLE L-LYSINE-EPSILON AMINOTRANSFERASE LAT (L-LYSINE AMINOTRAN	intermediary metabolism and respiration
Rv3297	nei	0,000144 6	0,004016 83	3681320	3682087	2,558707 122	PROBABLE ENDONUCLEASE VIII NEI	information pathways
Rv3335c	Rv3335c	2,77E-06	0,000137 7	3721731	3722500	2,542672978	PROBABLE CONSERVED INTEGRAL MEMBRANE PROTEIN	cell wall and cell processes
Rv3336c	trpS	5,14E-06	0,000252 3	3722621	3723831	2,065 216837	PROBABLE TRYPTOPHANYL-TRNA SYNTHETASE TRPS (TRYPTOPHAN--TRNA LIG	information pathways
Rv3360	Rv3360	8,12E-05	0,002484 5	3772651	3773016	2,183468659	CONSERVED HYPOTHETICAL PROTEIN	Conserved hypthetical s
Rv3370c	dnaE2	2,94E-09	2,81E-07	3781501	3784740	6,079385846	PROBABLE DNA POLYMERASE III (ALPHA CHAIN) DNAE2 (DNA NUCLEOTIDYLTR	information pathways
Rv3395c	Rv3395c	0,000190 2	0,005010 19	3811025	3811636	3,045567372	CONSERVED HYPOTHETICAL PROTEIN	Conserved hypthetical s
Rv3419c	gcp	1,72E-08	1,37E-06	3837555	3838586	2,637 190323	PROBABLE O-SIALOGLYCOPROTEIN ENDOPEPTIDASE GCP (GLYCOPROTEASE)	intermediary metabolism and respiration
Rv3420c	rimI	0,000020 68	0,001547 6	3838589	3839059	2,290559348	RIBOSOMAL-PROTEIN-ALANINE ACETYLTRANSFERASE RIMI (ACETYLATING EN	information pathways
Rv3422c	Rv3422c	8,02E-07	4,61E-05	3839694	3840194	2,429967253	CONSERVED HYPOTHETICAL PROTEIN	Conserved hypthetical s
Rv3484	cpsA	8,13E-10	8,45E-08	3903078	3904616	2,720488079	POSSIBLE CONSERVED PROTEIN CPSA	Conserved hypthetical s
Rv3529c	Rv3529c	0,000025 45	0,003388 5	3965884	3967038	2,576842729	CONSERVED HYPOTHETICAL PROTEIN	Conserved hypthetical s
Rv3538	Rv3538	4,27E-06	0,000199 2	3977052	3979722	2,596301055	PROBABLE DEHYDROGENASE. Possible 2-enoyl acyl-CoA hydratase.	intermediary metabolism and respiration
Rv3542c	Rv3542c	3,68E-05	0,001279 7	3981048	3981977	2,392347551	CONSERVED HYPOTHETICAL PROTEIN	lipid metabolism
Rv3552	Rv3552	3,06E-05	0,001409 13	3990774	3991523	2,758629665	POSSIBLE COA-TRANSFERASE (BETA SUBUNIT)	intermediary metabolism and respiration
Rv3567c	hsaB	3,84E-05	0,001783 2	4003719	4005282	2,537909384	POSSIBLE OXIDOREDUCTASE. Possible 3-hydroxy-9,10-secoandrost-1,3,5(10)-	intermediary metabolism and respiration
Rv3740c	Rv3740c	7,32E-65	3,38E-61	4190833	4192179	22,81796506	CONSERVED HYPOTHETICAL PROTEIN. POSSIBLE TRIACYLGLYCEROLSYNTHASE	lipid metabolism
Rv3741c	Rv3741c	3,75E-101	2,59E-97	4192179	4193650	115,9358364	POSSIBLE OXIDOREDUCTASE	intermediary metabolism and respiration
Rv3742c	Rv3742c	7,29E-127	1,01E-122	4192853	4193245	188,7788515	POSSIBLE OXIDOREDUCTASE	intermediary metabolism and respiration
Rv3757c	proW	3,06E-06	0,000151 2	4202613	4203287	2,563323434	POSSIBLE OSMOPROTECTANT (GLYCINE BETAINE/CARNITINE/CHOLINE)/L-PRO	cell wall and cell processes
Rv3758c	proV	0,000010 18	0,000123 72	4203299	4204417	2,048118421	POSSIBLE OSMOPROTECTANT (GLYCINE BETAINE/CARNITINE/CHOLINE)/L-PRO	cell wall and cell processes
Rv3776	Rv3776	3,60E-44	4,53E-41	4221089	4225581	11,24725392	CONSERVED HYPOTHETICAL PROTEIN	Conserved hypthetical s
Rv3870	eccCa1	3,64E-07	2,25E-05	4346481	4348724	2,117366046	ESX CONSERVED COMPONENT ECCCA1. POSSIBLE TRANSMEMBRANE PROTEIN	cell wall and cell processes
Rv3871	eccCb1	8,22E-08	5,80E-06	4348827	4350602	2,212783475	ESX CONSERVED COMPONENT ECCCB1	cell wall and cell processes

B. Down-regulated genes

id	transcript	pval	padj	start	stop	fold change	function	gene category
Rv1198	esxL	5,41E-22	1,92E-19	1341006	1341290	0,231348438	PUTATIVE ESAT-6 LIKE PROTEIN ESXL (ESAT-6 LIKE PROTEIN 8)	cell wall and cell processes
Rv1040c	PE8	3,27E-13	5,08E-11	1162549	1163376	0,257396826	PE FAMILY PROTEIN	PE/PPE
Rv0096	PPE1	8,75E-06	0,0003615	105324	106715	0,259235954	PPE FAMILY PROTEIN	PE/PPE
Rv1196	PPE18	7,25E-19	1,86E-16	1339349	1340524	0,261826652	PPE FAMILY PROTEIN	PE/PPE
Rv1960c	parD1	1,97E-08	1,54E-06	2203977	2204212	0,298615965	POSSIBLE ANTITOXIN PARD1	virulence, detoxification, adaptation
Rv0979A	rpmF	2,75E-08	2,08E-06	1094886	1095059	0,315282632	PROBABLE 50S RIBOSOMAL PROTEIN L32 RPMF	information pathways
Rv2628	Rv2628	0,0001084	0,0032041	2955058	2955420	0,330701702	HYPOTHETICAL PROTEIN	conserved hypotheticals
Rv0288	esxH	7,28E-13	1,11E-10	351848	352138	0,339492886	LOW MOLECULAR WEIGHT PROTEIN ANTIGEN 7 (ESXH) (10 kDa	cell wall and cell processes
Rv0287	esxG	4,25E-12	6,25E-10	351525	351818	0,351220102	ESAT-6 LIKE PROTEIN ESXG (CONSERVED HYPOTHETICAL PROTEI	cell wall and cell processes
Rv1197	esxK	0,0001107	0,0032372	1340659	1340955	0,36299103	ESAT-6 LIKE PROTEIN ESXK (ESAT-6 LIKE PROTEIN 3)	cell wall and cell processes
Rv1344	mbtL	0,0003265	0,0079232	1508968	1509281	0,379228765	PROBABLE ACYL CARRIER PROTEIN (ACP) MBTL	lipid metabolism
Rv3136	PPE51	3,82E-10	4,23E-08	3501794	3502936	0,386733947	PPE FAMILY PROTEIN	PE/PPE
Rv0285	PE5	1,55E-06	8,33E-05	349627	349932	0,441997265	PE FAMILY PROTEIN	PE/PPE
Rv3137	Rv3137	8,70E-06	0,0003612	3503393	3504175	0,451704469	PROBABLE MONOPHOSPHATASE	intermediary metabolism and respiration
Rv3198A	Rv3198A	0,0001174	0,0033909	3571335	3571589	0,45259865	POSSIBLE GLUTAREDOXIN PROTEIN	intermediary metabolism and respiration
Rv2346c	esxO	1,52E-07	1,01E-05	2625888	2626172	0,453305192	PUTATIVE ESAT-6 LIKE PROTEIN ESXO (ESAT-6 LIKE PROTEIN 5)	cell wall and cell processes
Rv0703	rplW	0,0003439	0,0083021	802133	802435	0,463563975	PROBABLE 50S RIBOSOMAL PROTEIN L23 RPLW	information pathways
Rv0099	fadD10	2,42E-05	0,0008861	108156	109778	0,4682323	POSSIBLE FATTY-ACID-CoA LIGASE FADD10 (FATTY-ACID-CoA SY	lipid metabolism
Rv0440	groEL2	3,23E-07	2,02E-05	528608	530230	0,473874656	60 kDa CHAPERONIN 2 (GROEL2) (PROTEIN CPN60-2) (GROEL2 PR	virulence, detoxification, adaptation
Rv2876	Rv2876	1,98E-05	0,0007328	3187663	3187977	0,481703808	POSSIBLE CONSERVED TRANSMEMBRANE PROTEIN	cell wall and cell processes
Rv0709	rpmC	7,30E-05	0,0022684	805526	805756	0,483791282	PROBABLE 50S RIBOSOMAL PROTEIN L29 RPMC	information pathways
Rv0652	rplL	5,00E-05	0,0016658	748849	749234	0,502683316	PROBABLE 50S RIBOSOMAL PROTEIN L7/L12 RPLL (SA1)	information pathways
Rv0572c	Rv0572c	1,16E-05	0,0004609	665042	665383	0,507537529	HYPOTHETICAL PROTEIN	conserved hypotheticals

Supplemental experimental procedures

Culture conditions and REMA assay of various bacteria. Mycobacteria (*Mycobacterium bovis* BCG*, M. marinum* strain M*, M. smegmatis MC^{2}155*) were grown in 7H9 broth (Difco) supplemented with Middlebrook albumin-dextrose-catalase (ADC) enrichment, 0.2% glycerol, 0.05% Tween 80. *Bacillus subtilis, Candida albicans, Corynebacterium glutamicum ATCC13032, Micrococcus luteus, Pseudomonas putida, Salmonella typhimurium* and *Staphylococcus aureus* were grown in Luria broth base (Sigma). *Corynebacterium diphtheriae, Enterococcus faecalis, Listeria monocytogenes* and *Pseudomonas aeruginosa* were grown in brain heart infusion broth (Difco). Two-fold serial dilutions of each test compound were prepared in 96-well plates containing bacteria in a total volume of 100 µl and then incubated at 37°C or 30°C (depend on the strain) before addition of 10 µl of 0.025% resazurin. After incubation, fluorescence of the resazurin metabolite resorufin was determined (excitation at 560 nm and emission at 590 nm, Gain 80) by using a TECAN Infinite M200 microplate reader.

Dimethyl Labeling and SAX fractionation and digestion of culture filtrate proteins. For the secretome analysis 10 µg of protein was reconstituted in 200 µl of 4 M Urea, 10% acetonitrile and buffered with Tris-HCl pH 8.5 to a final concentration of 30 mM. Proteins were reduced in 10 mM dithioerythritol (DTE) at 37°C for 60 min. and then alkylated in 40 mM iodoacetamide at 37°C for 45 min. Reactions were quenched by addition of DTE to a final concentration of 10 mM. First, protein digestion was performed using Lys-C (1:50 enzyme: protein) for 2 hours at 37°C. The lysates were then diluted 5-fold and a second digestion was performed overnight at 37°C using mass spectrometry grade trypsin gold (1:50 enzyme: protein) and 10 mM $CaCl_2$. Reactions were stopped by addition of 8 µl of pure formic acid and peptides were concentrated by vacuum centrifugation to a final volume of 70 µl. After digestions, samples were dimethyl-labeled as described previously (Boersema et al., 2009). In brief, culture filtrates from bacteria treated with DMSO were labeled with light dimethyl reactants (CH_2O + $NaBH_3CN$) and Culture filtrates from bacteria treated with BBH7 were labeled with medium reactants (CD_2O + $NaBH_3CN$). In the "reverse" experiment, the labelling of the culture filtrates from bacteria treated with DMSO and BBH7 samples were reversed. As a final step of labeling the procedure, samples were mixed in a 1: 1 (Light:Medium) and lyophilized.

SAX fractionation was performed as previously described with minor modifications (Wisniewski et al., 2009). Stage Tips were prepared by placing six layers of a 3M Empore™ anion exchange disk (3M) into a P200 pipette tips. SAX buffers were freshly prepared and titrated (pH 2, 4, 5, 6, 8, 11) with NaOH. Tips were first conditioned successively with 100% Methanol, 1M NaOH and Phosphoric acid buffer (pH 11). Samples were reconstituted in SAX buffer (pH 11) and loaded into the conditioned tips. The loading flow-through as well as the pH step elutions (in decreasing order of pH) were on-line captured on Empore™ C18 stage tips. Each collected fraction was washed with 0.1% TFA and eluted with acidified high organic content solvent. Eluted fractions were finally dried by vacuum centrifugation and used for LC-MS/MS analysis.

Mass Spectrometry and Data Analysis. Each SAX fraction was resuspended in 2% acetonitrile, 0.1% FA and loaded on a capillary pre-column (Magic AQ C18; 3µm by 200Å; 2 cm x 100 µm ID). Separations were performed on a C18 tip-capillary column (Nikkyo Technos Co; Magic AQ C18; 3µm by 100Å; 15 cm x 75 µm) using a Dionex Ultimate 3000 RSLC nano UPLC system. Data were acquired in data-dependent mode (over a 4 hr acetonitrile 2–42% gradient) on an Orbitrap Elite Mass spectrometer. Acquired RAW files were processed using MaxQuant version 1.3.0.5 (Cox et al., 2009) and its internal search engine Andromeda (Cox et al., 2011). The *Mtb* strain H37Rv R26 database (http://tuberculist.epfl.ch/) (Lew et al., 2011) was used for the search and MaxQuant default identification settings were applied in combination with specific dimethyl labeling parameters. Search results were filtered with a false-discovery rate of 0.01. Known contaminants and reverse hits were removed before statistical analysis. Relative quantification within different conditions was obtained calculating the significance B values for each of the identified proteins using Perseus (Cox et al., 2009).

Genome annotation and RNA-seq data analysis. All analyses in this study were carried out using the *M. tuberculosis* H37Rv annotation from the TubercuList database (http://tuberculist.epfl.ch/) (Lew et al., 2011). There are 4019 protein coding sequences (CDS) currently annotated in the genome, 73 genes encoding for stable RNAs, small RNAs and tRNAs. In order to quantify protein occupancy and transcription across the entire genome, 3080 intergenic regions (regions flanked by two non-overlapping CDS) were included, resulting in a total of 7172 features.

The single-ended sequence reads generated from RNA-seq experiments were aligned to the *M. tuberculosis* H37Rv genome (NCBI accession NC_000962.2) using Bowtie2 with default parameters (Langmead and Salzberg, 2012). Read counts for all annotated features were obtained with the htseq-count program (http://www-huber.embl.de/users/anders/HTSeq/doc/count.html). Regions where genes overlapped were excluded from counting. Reads spanning more than one feature were counted for each feature. Since the RNA library was strand-specific, the orientation of sequence reads had to correspond to the orientation of annotated features to be counted. Analysis of differential gene expression was carried out using the DESeq package (Anders and Huber, 2010).

Cloning and purification of His_6-tagged MprB. Cloning of the *mpr*B PCR-product into pQE80L (Qiagen) was performed using the In-Fusion PCR Cloning kit (Clontech). Two litres of mid-log phase *E. coli* BL21 (DE3) culture were induced with 0.5 mM isopropyl β-d-thiogalactoside (IPTG) and incubated for 12 hours at 16°C. cells were lysed in lysis buffer (50 mM Tris pH 8, 500 mM NaCl, 5 mM imidazole, 10% glycerol, 1% Tween 20) using a French press. After clearance by centrifugation, the lysates were incubated with 1 g of PrepEase resin (USB, Cleveland, USA) for 1 hour at 4°C followed by separation on a PolyPrep chromatography column (Biorad). The resin was washed with two column volumes of buffer containing 10 mM imidazole and eluted with 250 mM imidazole. After dialysis against 25 mM Tris pH7.5 and 200 mM NaCl the protein was further purified by gel filtration on a HiLoad 16/60 Superdex 200 column (Amersham Biosciences).

Data processing for intracellular quantification of bacteria using confocal microscopy. For quantification of intracellular bacteria the DAPI-channel was filtered using a median filter of 2 pixels (radius), and a Gaussian blur with a sigma of 2 pixels. Afterwards, an automatic threshold using Huang's fuzzy thresholding method (Fiji, “Huang” auto threshold) was applied on this modified image of the DAPI-channel and an automatic threshold using Tsai's thresholding method (Fiji, "Moments" auto threshold) was applied on the bacteria-channel. Finally, the area of each segmented image was measured. Areas or their ratio can be plotted and are indicative of the bacterial load within macrophage.

Synthesis of BTP15 and BBH7

Synthesis of BTP15 (5-Bromo-2-(cyclopropanecarbonyl-amino)-6-hydroxy-benzo[b]thiophene-3-carboxylic acid amide)

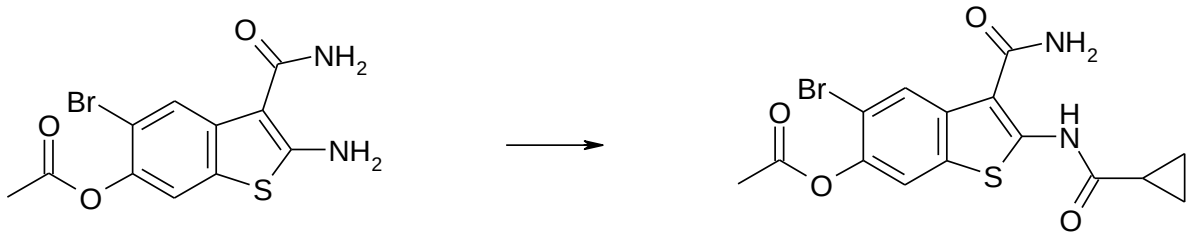

The solution of 0.33 g (1 mmol) acetic acid 2-amino-5-bromo-3-carbamoyl-benzo[b]thiophen-6-yl ester (HU P1300338) in 10 cm^3 pyridine at 0 °C was treated drop wise with 0.12 g, 0.10 cm^3 (1.10 mmol) cylopropylcarbonylchloride. The reaction mixture was stirred at room temperature (RT) for five hours, and then was evaporated under vacuum. The residue was stirred in 15 cm^3 1 N water solution of hydrochloride acid at RT for 30 minutes, then the product was filtered off and was washed with water. The crude product was refluxed in 10 cm^3 ethanol for half an hour, it was cooled to 0 °C and the pure product was filtered off.

Yield: 0.30 g (75 %)

^{1}H-NMR (DMSO-d6): 11.80 (s, 1H), 7.95 (s, 1H), 7.70 (bs, 2H), 7.35 (s, 1H), 1.98 (m, 1H), 0.91 (m, 4H) ppm.

LC-MS: M^-= 395

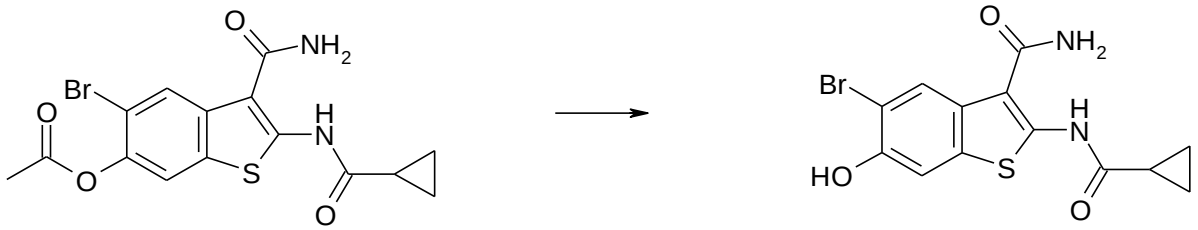

The solution of 0.20 g (0.50 mmol) acetic acid 5-bromo-3-carbamoyl-2-(cyclopropanecarbonyl-amino)-benzo[b]thiophen-6-yl ester in 30 cm^3 methanol at RT was treated in one portion with a 1.00 cm^3 (2.00 mmol) water solution of sodium

hydroxide. The reaction mixture was stirred at RT for two hours, and then was evaporated under vacuum. The residue was stirred in 15 cm^3 1 N water solution of hydrochloride acid at RT for half an hour, then the product was filtered off and was washed with water. The crude product was refluxed in 10 cm^3 acetonitrile for half an hour, it was cooled to 0°C and the pure product was filtered off.

Yield: 0.14 g (77 %)

^{1}H-NMR (DMSO-d6): 11.80 (s, 1H), 10.32 (s, 1H), 7.98 (s, 1H), 7.74 (bs, 2H), 7.38 (s, 1H), 1.98 (m, 1H), 0.91 (m, 4H) ppm.

LC-MS: M^-= 353

Synthesis of BBH7 (4)

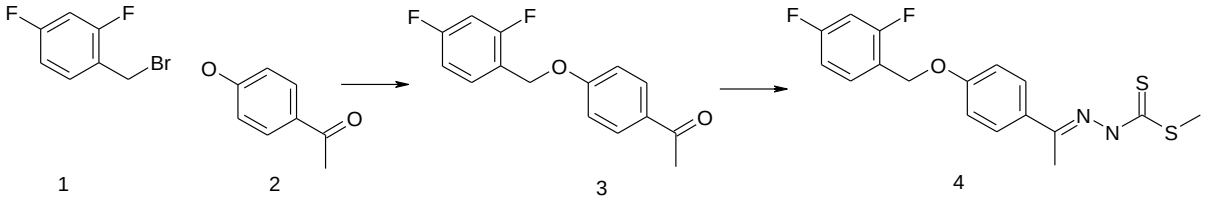

1 2 3 4

1-[4-(2,4-Difluoro-benzyloxy)-phenyl]-ethanone (3)

The mixture of 2,4-difluorobenzyl bromide (**1**, 6.00 g, 29 mmol), acetone (45 ml), potassium carbonate (2.18 g, 16 mmol), potassium iodide (100 mg) and 4′-hydroxyacetophenone (**2**, 4.08 g, 30 mmol) was stirred at reflux temperature for 24 hours. The inorganic salts were filtered off, washed with acetone then the filtrate was evaporated in vacuum. The residue was taken up in the mixture of chloroform (30 ml) and aqueous sodium hydroxide solution (10 wt%, 20 ml). The two layers were separated; the aqueous layer was extracted two times with chloroform (2 x 20 ml). The organic layers were combined, washed with water, dried on sodium sulfate, and evaporated in vacuum. The residue was solidified under hexane. The precipitate was filtered washed with hexane then dried on air. Thus 6.64 g of the title compound (**3**) was obtained. Yield: 87%

$C_{15}H_{12}F_2O_2$, Mw=262.26, Exact Mass =262.08

LC-MS purity: 99 % m/z 263 $[M]^+$, Rt. 4.24 min.

^{1}H-NMR in DMSO-d_6 δ: 7.94 (dm, *J* = 8.8 Hz, 2H), 7.65 (ddd, *J* = 8.7, 8.7 and 6.8 Hz, 1H), 7.32 (ddd, *J* = 10.6, 9.4 and 2.5 Hz, 1H), 7.15 (dddd, *J* = 8.7, 8.7, 2.5 and 1.0 Hz, 1H), 7.14 (dm, *J* = 8.8 Hz, 2H), 5.21 (s, 2H), 2.52 (s, 3H)

N'-{1-[4-(2,4-Difluoro-benzyloxy)-phenyl]-ethylidene}-hydrazinecarbodithioic acid methyl ester (4)

The mixture of 1-[4-(2,4-difluoro-benzyloxy)-phenyl]-ethanone (**3**, 1.57 g, 6.00 mmol), hydrazinecarbodithioic acid methyl ester (732 mg, 6.00 mmol) and acetic acid (20 ml) was stirred at room temperature for 24 hours. The precipitate was filtered off, washed with acetic acid then with diisopropyl ether and dried under vacuum. Thus 1.68 g of the title compound (**4**) was obtained. Yield: 76%

$C_{17}H_{16}F_2N_2OS_2$, Mw=366.45, Exact Mass =366.07

LC-MS purity: 99 %, m/z 365 $[M-H]^-$, 367 $[M]^+$ Rt. 4.90 min.

^{1}H-NMR in DMSO-d_6 δ: 12.35 (s, 1H), 7.83 (dm, *J* = 8.8 Hz, 2H), 7.64 (ddd, *J* = 9.0, 8.3 and 6.4 Hz, 1H), 7.31 (ddd, *J* = 10.1, 10.0 and 1.9 Hz, 1H), 7.14 (dddd, *J* = 9.0, 8.3, 1.9 and 1.0 Hz, 1H), 7.09 (dm, *J* = 8.8 Hz, 2H), 5.17 (s, 2H), 2.50 (s, 3H), 2.35 (s, 3H)

^{13}C-NMR δ: 199.5, 162.0 ($J_{C,F}$ = 247.0 and 12.8 Hz), 160.5 ($J_{C,F}$ = 248.0 and 12.8 Hz), 159.8, 151.7, 132.4 ($J_{C,F}$ = 10.3 and 5.2 Hz), 130.2, 128.3, 120.2 ($J_{C,F}$ = 14.9 and 3.8 Hz), 114.8, 111.8 ($J_{C,F}$ = 21.3 and 3.6 Hz), 104.2 ($J_{C,F}$ = 25.6 and 25.6 Hz), 63.4, ($J_{C,F}$ = 2.3 Hz), 17.1, 14.6

The signal assignation is based on HSQC and HMBC experiments.

The *E* isomer is proven by crosspeaks between the NH (12.35 ppm) and the C-CH_3 (2.35 ppm) signals observed in the ROESY spectrum

Oligonucleotides used in this study

TCACCATCACGGATCCACCGAAGCGGCCGAG	Product for pQE80L::mprB
TCAGCTAATTAAGCTTCTAGGTTGCGCGCGT	
AAAGGGGTTGATCTCGTGAC	qRTPCR phoP
GTTGGTCGCGGTGTAGACTT	
TGGTCTGGTTGACTTGCTTG	qRTPCR dosR
ATCTAGCATGGCCTCGTCAG	
CGAACGGCTTTGGTAGGTAG	qRTPCR mprA
CGAACGGCTTTGGTAGGTAG	
CGTTCGCATCGACGTAGTAG	qRTPCR hrp1
CGTTCGCATCGACGTAGTAG	
CCCGAGTTTTCTGAGCTGTT	qRTPCR hspX
TAATGTCGACGTCCTTGTCG	
GATCGAAGCAGCGGTGAC	qRTPCR nrdZ
GCTGCCGGTAGATGATGTAAA	
GGGTTTCTCAAGGCAGAAGA	qRTPCR tgs1
AAGATCGAAGTCGGGATCGT	
CAACCAAGGGGGTATCCTTT	qRTPCR espA
CTGATGAGCTGACGATCGAG	
ACTGTAGTTGACGCCGAGGT	qRTPCR ctpG
ATTGCGCGTGAATACCAGAT	
ACCTGGTGGACAACTCGATG	qRTPCR lpqS
GAACCGGGTCAACAGGTCT	
CAGCTCGGAGATCCACTCAC	qRTPCR ctpC
TTGGACACCCGAACTTTTTC	
CGAAGACGTGATCACTGAGG	qRTPCR eccA5
AGATCCTCATCGTCCAAACG	
CAGGCTTACAAGGCAACCAT	qRTPCR eccCb1
TTCTTCTGGAGGCTCGATGT	
TTCAGCTAGCCCTCAACGTC	qRTPCR cadI
GACTTCCACACCGAGATGGT	
CCTTTGGCCTACAGCTCATC	qRTPCR dnaE2
TAGCCCGGAAATCTCAGTTG	

GCACCATGGTTGGCAATAC	qRTPCR cysK2
CCACCGGTTGATTCGACTAT	
ATCATCCTCGACGATTGGAC	qRTPCR mmcO
ATTCGCCCGTTGATCAGATA	
ACGACGTGGGTCAGGTACTC	qRTPCR csd
ACGCTCTTCCAAAGAAATGC	
TGTGTCCAACCATCTGTCGT	qRTPCR csd
ACACAGGGTTGGTCGGTATC	
GAGCGCAAGGGCTACCTAC	qRTPCR lexA
ACGTCTTCAACGGCTTCCT	
GAGGGTGATACGAATGACGAA	qRTPCR mymT
CACAGTGGCATGGGACTTC	
TTGGATGCTCATATCCCACA	qRTPCR esxG
CCAACAAGGTGTTGACTTTGG	
ATGACGTTGCGAGTGGTTC	qRTPCR pe5
CAGCTCTTCGACACCTTCG	
CTGACAGAGGCATTCAATTT	qRTPCR mprB
ATCAAGAGTTCGACATTGGT	

Supplemental references

Anders, S., and Huber, W. (2010). Differential expression analysis for sequence count data. Genome Biol *11*, R106.

Boersema, P.J., Raijmakers, R., Lemeer, S., Mohammed, S., and Heck, A.J. (2009). Multiplex peptide stable isotope dimethyl labeling for quantitative proteomics. Nat Protoc *4*, 484-494.

Cox, J., Matic, I., Hilger, M., Nagaraj, N., Selbach, M., Olsen, J.V., and Mann, M. (2009). A practical guide to the MaxQuant computational platform for SILAC-based quantitative proteomics. Nat Protoc *4*, 698-705.

Cox, J., Neuhauser, N., Michalski, A., Scheltema, R.A., Olsen, J.V., and Mann, M. (2011). Andromeda: a peptide search engine integrated into the MaxQuant environment. J Proteome Res *10*, 1794-1805.

He, H., Hovey, R., Kane, J., Singh, V., and Zahrt, T.C. (2006). MprAB is a stress-responsive two-component system that directly regulates expression of sigma factors SigB and SigE in Mycobacterium tuberculosis. Journal of bacteriology *188*, 2134-2143.

Langmead, B., and Salzberg, S.L. (2012). Fast gapped-read alignment with Bowtie 2. Nat Methods *9*, 357-359.

Lew, J.M., Kapopoulou, A., Jones, L.M., and Cole, S.T. (2011). TubercuList--10 years after. Tuberculosis (Edinb) *91*, 1-7.

Pang, X., Vu, P., Byrd, T.F., Ghanny, S., Soteropoulos, P., Mukamolova, G.V., Wu, S., Samten, B., and Howard, S.T. (2007). Evidence for complex interactions of stress-associated regulons in an mprAB deletion mutant of Mycobacterium tuberculosis. Microbiology *153*, 1229-1242.

Wisniewski, J.R., Zougman, A., and Mann, M. (2009). Combination of FASP and StageTip-based fractionation allows in-depth analysis of the hippocampal membrane proteome. J Proteome Res *8*, 5674-5678.

Zhang, J.H., Chung, T.D., and Oldenburg, K.R. (1999). A Simple Statistical Parameter for Use in Evaluation and Validation of High Throughput Screening Assays. J Biomol Screen *4*, 67-73.